1-1-2015

Asymptotic Analysis of The SVD For The Truncated Hilbert Transform With Overlap

Reema Al-Aifari

Michel Defrise

Alexander Katsevich
University of Central Florida

SIAM J. MATH. ANAL.
Vol. 47, No. 1, pp. 797–824

ASYMPTOTIC ANALYSIS OF THE SVD FOR THE TRUNCATED HILBERT TRANSFORM WITH OVERLAP*

RIMA ALAIFARI†, MICHEL DEFRISE‡, AND ALEXANDER KATSEVICH§

Abstract. The truncated Hilbert transform with overlap H_T is an operator that arises in tomographic reconstruction from limited data, more precisely in the method of differentiated back-projection. Recent work [R. Al-Aifari and A. Katsevich, *SIAM J. Math. Anal.*, 46 (2014), pp. 192–213] has shown that the singular values of this operator accumulate at both zero and one. To better understand the properties of the operator and, in particular, the ill-posedness of the inverse problem associated with it, it is of interest to know the rates at which the singular values approach zero and one. In this paper, we exploit the property that H_T commutes with a second-order differential operator L_S and the global asymptotic behavior of its eigenfunctions to find the asymptotics of the singular values and singular functions of H_T.

Key words. limited data, computerized tomography, spectrum, asymptotic analysis, Hilbert transform, ill-posedness

AMS subject classifications. 34E20, 45Q05, 47A10, 47A75, 34B24, 44A12

DOI. 10.1137/140952296

1. Introduction.

In two-dimensional or three-dimensional computerized tomography, an image of an object is reconstructed from measurements that can be modeled as Radon transform or cone beam transform data, respectively. Typically, a source emitting a beam of X-rays rotates around the object and a detector measures the attenuation of the X-ray beam after it traverses the object. When measurements from a sufficiently dense set of rays crossing the object are collected, standard techniques (e.g., filtered back-projection) allow for stable reconstruction [12].

In the case of limited data, e.g., when only measurements from an angular range less than 180 degrees are available or when only a strict subset of the object support is illuminated from all directions, reconstruction becomes more difficult. While these cases can occur in practice (for example, with an oversize patient), reconstruction from limited data may also allow reduction of the radiation dose to which patients are exposed.

The differentiated back-projection, a method based on a result by Gelfand and Graev [7], allows one to identify a class of limited data configurations, such that reconstruction is still possible. It is based on the reduction of the two- or three-dimensional problem to a family of one-dimensional problems. These consist of the reconstruction of a compactly supported function in one dimension from its partially known Hilbert transform. The application of the Gelfand–Graev formula to tomography was first

*Received by the editors January 10, 2014; accepted for publication (in revised form) October 6, 2014; published electronically February 19, 2015.
http://www.siam.org/journals/sima/47-1/95229.html
†Seminar for Applied Mathematics, ETH Zürich, 8092 Zürich, Switzerland (rima.alaifari@sam.math.ethz.ch). The research of this author was supported by a fellowship from the Research Foundation Flanders (FWO).
‡Department of Nuclear Medicine, Vrije Universiteit Brussel, Brussels B-1090, Belgium (mdefrise@ulb.ac.be).
§Department of Mathematics, University of Central Florida, Orlando, FL 32816 (alexander.katsevich@ucf.edu). The research of this author was supported in part by NSF grants DMS-1115615 and DMS-1211164.

introduced by Finch [5] and later made explicit for two dimensions [13, 16, 19] and for three dimensions [14, 17, 18, 20].

In two dimensions, the differentiated back-projection reduces the reconstruction problem to a family of one-dimensional problems that can be formulated as inverting operators of the form $\mathcal{P}_{\Omega_1} H \mathcal{P}_{\Omega_2}$, where H is the Hilbert transform on $L^2(\mathbb{R})$; Ω_1, Ω_2 are finite intervals on $\mathbb{R}$; and $\mathcal{P}_\Omega$ is the projection operator $(\mathcal{P}_\Omega f)(x) = f(x)$ if $x \in \Omega$, or $(\mathcal{P}_\Omega f)(x) = 0$ otherwise. If $\Omega_2 \subset \Omega_1$, i.e., the Hilbert transform is measured on an interval covering the support of the object, the inversion of $\mathcal{P}_{\Omega_1} H \mathcal{P}_{\Omega_2}$ is well-posed and an explicit inversion formula is known [15].

In general, when $\Omega_2 \not\subset \Omega_1$ the inversion of $\mathcal{P}_{\Omega_1} H \mathcal{P}_{\Omega_2}$ has turned out to be *severely* ill-posed. Thus, it is of interest to study the singular value decomposition (SVD) of such operators. The SVD in the case of $\Omega_1 \subset \Omega_2$, which occurs in the so-called interior problem, has been studied in [9]. The SVD of the truncated Hilbert transform *with a gap*, which describes the case $\Omega_1 \cap \Omega_2 = \emptyset$, has been the subject of [8]. For both cases, the asymptotic behavior of the singular values and singular functions has been found in [10].

This paper concerns a different setup, the truncated Hilbert transform *with overlap* H_T. This is the case when the two intervals overlap, i.e., $\Omega_1 = [a_1, a_3]$, $\Omega_2 = [a_2, a_4]$ for real numbers $a_1 < a_2 < a_3 < a_4$. For this case, a uniqueness and *pointwise* stability result for the inversion was obtained in [3]. The SVD of the truncated Hilbert transform *with overlap* has been characterized in [1], where it is shown that the singular values of H_T accumulate at both 0 and 1. The accumulation point 0 causes the ill-posedness of inverting the operator H_T. Motivated by these results, this paper studies the asymptotic behavior of the singular values and singular functions of H_T. We prove (Theorems 5.3 and 6.1) that the singular values σ_n tend to the accumulation points 0 and 1 exponentially as

$$\sigma_n = 2e^{-n\pi K_+/K_-}\left(1 + \mathcal{O}(n^{-1/2+\delta})\right), \qquad n \to \infty,$$
$$\sigma_{-n} = \left(1 - 2e^{-2n\pi K_-/K_+}\right)\left(1 + \mathcal{O}(n^{-1/2+\delta})\right), \quad n \to \infty,$$

for some constants K_+ and K_- depending on the points a_1, a_2, a_3, a_4. The paper also describes the asymptotic behavior of the singular functions in terms of their Wentzel–Kramer–Brillouin (WKB) approximation away from the points a_1, a_2, a_3, a_4 and in terms of Bessel functions in a neighborhood of these points. Uniform expansions of the singular functions are obtained by matching the WKB and Bessel approximations in an overlap region.

The paper is organized as follows. Section 2 starts with an overview of the results obtained in [1] that will be used in the paper. In section 3 we show an intermediate result on the eigenvalues of a differential operator that is related to the operator H_T in a sense to be defined in section 2. Next, section 4 gives an outline and description of the approach used to find the asymptotic behavior of the SVD. In section 5, the asymptotic behavior of the SVD is derived for the subsequence of singular values accumulating at zero. We use this result together with a symmetry property in section 6 to obtain the asymptotics for the case where the singular values tend to 1. We conclude by comparing the theoretical results obtained from the asymptotic analysis with a numerical example in section 7.

2. Preliminaries. In [1] we have analyzed the spectrum of the operator $H_T^* H_T$, where $H_T : L^2([a_2, a_4]) \to L^2([a_1, a_3])$ is the truncated Hilbert transform *with overlap* defined for any fixed four real numbers $a_1 < a_2 < a_3 < a_4$ to be the following operator:

$$(H_T f)(x) := \frac{1}{\pi}\text{p.v.} \int_{a_2}^{a_4} \frac{f(y)}{y-x}dy, \quad x \in (a_1, a_3), \tag{2.1}$$

where p.v. stands for the principal value.

By relating H_T to a self-adjoint extension of a differential operator with which it commutes, we found that the singular values of H_T accumulate (only) at 0 and 1, where 0 and 1 themselves are not singular values. A natural question that then arises is the asymptotic behavior of the singular values, i.e., the convergence rates of the accumulation at 0 and 1. Especially in view of the ill-posedness of the inversion of H_T, it is important to ask how fast the singular values decay to zero.

To answer this question, we will need to consider the SVD $\{f_n, g_n; \sigma_n\}$, $n \in \mathbb{Z}$, of H_T,

$$H_T f_n = \sigma_n g_n, \tag{2.2}$$

$$H_T^* g_n = \sigma_n f_n, \tag{2.3}$$

and study the asymptotic behavior of the singular functions f_n and g_n to find the asymptotics of σ_n. For the indices of the singular values we choose the convention $n \to +\infty$ for $\sigma_n \to 0$ and $n \to -\infty$ for $\sigma_n \to 1$.

In what follows, we briefly summarize results found in [1], to which we refer for detail and proofs. By the commutation property, $\{f_n\}_{n\in\mathbb{Z}}$ are the eigenfunctions of the differential operator L_S that we define by first introducing

$$L(x, d_x)\psi(x) := (P(x)\psi'(x))' + 2(x-\sigma)^2\psi(x), \tag{2.4}$$

where

$$P(x) = \prod_{j=1}^{4}(x - a_j), \quad \sigma = \frac{1}{4}\sum_{j=1}^{4} a_j. \tag{2.5}$$

Let $D_{\max}$ denote the maximal domain on $(a_2, a_3) \cup (a_3, a_4)$ associated with $L(x, d_x)$ given by

$$\begin{aligned} D_{\max} := \{\ \psi : (a_2, a_3) \cup (a_3, a_4) \to \mathbb{C} : \psi_{2,3}, P\psi'_{2,3} \in AC_{loc}((a_2, a_3)), \\ \psi_{3,4}, P\psi'_{3,4} \in AC_{loc}((a_3, a_4)); \psi, L\psi \in L^2([a_2, a_4])\}, \end{aligned} \tag{2.6}$$

where $\psi_{2,3}$, $\psi_{3,4}$ denote the restrictions of ψ to (a_2, a_3) and (a_3, a_4), respectively, and $AC_{loc}(I)$ stands for the space of locally absolutely continuous functions on I. Furthermore, we introduce the notation $a_j^{\pm} = \lim_{\epsilon\to 0^{\pm}} a_j + \epsilon$ and the Lagrange sesquilinear form of two functions u, v:

$$[u, v] := uP\overline{v}' - \overline{v}Pu'.$$

Then, the realization $L_S : D(L_S) \to L^2([a_2, a_4])$ of $L(x, d_x)$ on the domain

$$\begin{aligned} D(L_S) := \{\psi \in D_{\max} : [\psi, u](a_2^+) = [\psi, u](a_4^-) = 0, \\ [\psi, u](a_3^-) = [\psi, u](a_3^+), [\psi, v](a_3^-) = [\psi, v](a_3^+)\} \end{aligned} \tag{2.7}$$

with the choice of maximal domain functions $u, v \in D_{\max}$

$$u(y) := 1, \tag{2.8}$$

$$v(y) := \sum_{i=1}^{4} \prod_{\substack{j \neq i \\ j\in\{1,\ldots,4\}}} \frac{1}{a_i - a_j} \ln|y - a_i| \tag{2.9}$$

is self-adjoint. The spectrum of L_S is real and discrete and the left singular functions f_n, $n \in \mathbb{Z}$, of H_T are the eigenfunctions of L_S,

$$L_S f_n = \lambda_n f_n, \tag{2.10}$$

and form an orthonormal basis of $L^2([a_2, a_4])$. For the differential operator $\tilde{L}_S : D(\tilde{L}_S) \subset L^2([a_1, a_3]) \to L^2([a_1, a_3])$, defined in the same way as L_S, but with a_2, a_3, a_4 replaced by a_1, a_2, a_3 in the definitions (2.6) and (2.7), we also obtain

$$\tilde{L}_S g_n = \lambda_n g_n. \tag{2.11}$$

Here, g_n are the right singular functions of H_T as in (2.2) and (2.3). The eigenvalues λ_n in (2.10) and (2.11) coincide. These properties allow us to formulate the following commutation relation:

$$H_T L_S = \tilde{L}_S H_T. \tag{2.12}$$

From the theory of Fuchs and Frobenius, it follows that the points a_i are *regular singular* and that the two linearly independent solutions to $(L-\lambda)\psi = 0$ in a neighborhood of a_i^+ or a_i^- are given by

$$\psi_1(x) = \sum_{n=0}^{\infty} b_n (x - a_i)^n, \tag{2.13}$$

$$\psi_2(x) = \sum_{n=0}^{\infty} d_n (x - a_i)^n + \ln|x - a_i| \psi_1(x), \tag{2.14}$$

where the coefficients d_n are different to the left and to the right of a_i. This allows us to simplify the characterization of the eigenfunctions f_n, $n \in \mathbb{Z}$, as follows: A function $f \in L^2([a_2, a_4])$ is an eigenfunction of L_S if and only if

- it solves $Lf = \lambda f$ for some $\lambda \in \mathbb{C}$,
- it is bounded at a_2^+ and at a_4^-,
- it is of the form $\phi_{11}(x) + \ln|x - a_3| \cdot \phi_{12}(x)$ at a_3^- and
- of the form $\phi_{21}(x) + \ln|x - a_3| \cdot \phi_{22}(x)$ at a_3^+ and
- with analytic functions ϕ_{ij} such that $\phi_{11}(x)$ matches $\phi_{21}(x)$ continuously at a_3 and $\phi_{12}(x)$ matches $\phi_{22}(x)$ continuously at a_3, i.e.,

$$\lim_{x \to a_3^-} \phi_{11}(x) = \lim_{x \to a_3^+} \phi_{21}(x), \tag{2.15}$$

$$\lim_{x \to a_3^-} \phi_{12}(x) = \lim_{x \to a_3^+} \phi_{22}(x). \tag{2.16}$$

We refer to (2.15), (2.16) as transmission conditions at the point a_3.

At a_i an eigenfunction g of $\tilde{L}_S$ satisfies the same conditions that an eigenfunction of L_S has at a_{i+1}, $i = 1, 2, 3$.

3. The spectrum of L_S has two accumulation points.

In [1], we have shown that the operator $(L_S - i)^{-1}$ is compact. Hence, the spectrum of L_S is purely discrete and the only possible accumulation points are $\lambda_n \to \pm\infty$, $n \in \mathbb{Z}$. As we will see in the following sections, deriving the asymptotics of the singular values σ_n of H_T for just one of the two possible accumulation points for λ_n results in only one accumulation point of σ_n. More precisely, $\lambda_n \to +\infty$ leads to $\sigma_n \to 0$ and $\lambda_n \to -\infty$ to $\sigma_n \to 1$.

Since we have shown in [1] that both 0 and 1 are accumulation points of the spectrum of $H_T^* H_T$, this suggests that the eigenvalues λ_n of L_S accumulate at both $+\infty$ and $-\infty$.

For self-adjoint realizations of $L(x, d_x)$ on an interval where the function $P(x)$ is negative, the spectrum of this self-adjoint realization is bounded below, but not above. Since in the case of L_S, we consider $P(x)$ on (a_2, a_4), i.e., on an interval on which P changes sign, it seems intuitive to assume that the spectrum of L_S is unbounded from below and from above.

Indeed, in the case where $P(x)$ changes sign and $1/P(x)$ is locally integrable on (a_2, a_4), standard results in Sturm–Liouville theory state that the spectrum of the resulting differential operator is unbounded from below and from above [11]. However, local integrability of $1/P(x)$ is not the case for L_S. In order to show the unboundedness from below and from above of the spectrum of L_S, we construct two sequences of functions $u_n \in D(L_S)$, $n \in \mathbb{N}$, supported on $[a_2, a_3]$ and $v_n \in D(L_S)$, $n \in \mathbb{N}$, supported on $[a_3, a_4]$ for which

$$\langle L_S u_n, u_n\rangle / \langle u_n, u_n\rangle \to -\infty, \tag{3.1}$$

$$\langle L_S v_n, v_n\rangle / \langle v_n, v_n\rangle \to +\infty, \tag{3.2}$$

as $n \to \infty$. For $I \subset \mathbb{R}$, let χ_I denote the characteristic function on I and define $w_1(x) = \chi_{[a_2,a_3]}(x)(x - a_2)(a_3 - x)$ and $w_2(x) = \chi_{[a_3,a_4]}(x - a_3)(a_4 - x)$. Then, we choose the functions u_n and v_n to be

$$u_n(x) := w_1(x)\cos(nx),$$
$$v_n(x) := w_2(x)\cos(nx).$$

From $(P(x)u_n'(x))' = -P(x)w_1(x)n^2\cos(nx) + \mathcal{O}(n)$, we obtain

$$\begin{aligned}\langle L_S u_n, u_n\rangle &= -n^2 \int_{a_2}^{a_3} P(x) w_1^2(x)\cos^2(nx)dx + \mathcal{O}(n) \\ &\le -n^2(a_2 - a_1)(a_4 - a_3)\int_{a_2}^{a_3} w_1^3(x)\cos^2(nx)dx + \mathcal{O}(n).\end{aligned} \tag{3.3}$$

A direct computation yields

$$\int_{a_2}^{a_3} ((x - a_2)(a_3 - x))^3 \cos^2(nx)dx = \frac{(a_3 - a_2)^7}{280} + \mathcal{O}(n^{-4})$$

so that the integral on the right-hand side in (3.3) is bounded away from zero. Thus, $\langle L_S u_n, u_n\rangle \to -\infty$. Furthermore, from $\|u_n\|_{L^2} \le \|w_1\|_{L^2}$, we find that (3.1) holds.

Similarly, we get for v_n that $(P(x)v_n'(x))' = -P(x)w_2(x)n^2\cos(nx) + \mathcal{O}(n)$ and

$$\begin{aligned}\langle L_S v_n, v_n\rangle &= -n^2 \int_{a_3}^{a_4} P(x) w_2^2(x)\cos^2(nx)dx + \mathcal{O}(n) \\ &\ge n^2(a_3 - a_1)(a_3 - a_2)\int_{a_3}^{a_4} w_2^3(x)\cos^2(nx)dx + \mathcal{O}(n).\end{aligned} \tag{3.4}$$

Moreover,

$$\int_{a_3}^{a_4} ((x - a_3)(a_4 - x))^3 \cos^2(nx)dx = \frac{(a_4 - a_3)^7}{280} + \mathcal{O}(n^{-4}).$$

Therefore, $\langle L_S v_n, v_n\rangle \to +\infty$. The inequality $\|v_n\|_{L^2} \le \|w_2\|_{L^2}$ then implies (3.2).

THEOREM 3.1. *The spectrum of L_S is purely discrete and accumulates at $+\infty$ and $-\infty$, i.e., the operator is unbounded from below and from above. There are no further accumulation points in the spectrum.*

Remark 3.2. The singular functions f_n and g_n of H_T are the nth eigenfunctions of the operators L_S and $\tilde{L}_S$, respectively. The spectra of L_S and $\tilde{L}_S$ are the same, i.e.,

$$L_S f_n = \lambda_n f_n,$$
$$\tilde{L}_S g_n = \lambda_n g_n.$$

The above theorem states that the eigenvalues λ_n accumulate at both $+\infty$ and $-\infty$. As a consequence (see, e.g., [4, section 4.5]), when λ_n is large and positive, the functions f_n oscillate on the region where $P(x)$ is negative and decay monotonically where $P(x)$ is positive. The same is true for g_n. Thus, the f_n are oscillatory on (a_3, a_4), the g_n oscillate on (a_1, a_2), and they are both monotonic on (a_2, a_3). The opposite is true for large negative λ_n. In this case, f_n and g_n both oscillate on (a_2, a_3) and are monotonic outside of this interval. This corresponds to singular values σ_n of H_T close to 1 and means that when inverting H_T, high frequencies of the solution can be well recovered, if they occur in the region (a_2, a_3). The case $\lambda_n \to +\infty$ corresponds to $\sigma_n \to 0$. Thus, high frequencies of the solution on (a_3, a_4) cannot be recovered stably. Figure 1 shows a plot of the singular functions f_n and g_n for both cases.

4. A procedure for finding the asymptotics of the singular functions.

We now want to study the asymptotic behavior of the eigenfunctions f_n of L_S and g_n of $\tilde{L}_S$ as $\lambda_n \to +\infty$. In section 6 we will treat the case $\lambda_n \to -\infty$. Away from the singular points a_i the solutions to the Sturm–Liouville problem for large eigenvalues are well approximated by the WKB method (see [2]). Close to the singularities, the solutions can be estimated by Bessel functions of the first and the second kind. These two local asymptotic expansions can then be matched in the overlap of their regions of validity. This procedure was introduced for two other instances of the truncated Hilbert transform—the interior problem and the truncated Hilbert transform *with a gap*—in [10], to which we refer for full detail and proofs. The difficulty here lies in the essential difference between the Sturm–Liouville problems for L_S and $\tilde{L}_S$ and the cases considered in [10]. This is due to the presence of singular points a_3 and a_2 in the interior of (a_2, a_4) and (a_1, a_3), respectively.

4.1. Outline of the construction of g_n for $\lambda_n \to +\infty$.

First, we start with a solution $\phi = g$ to

$$(L - \lambda)\phi = 0 \tag{4.1}$$

on (a_1, a_2) and then require that it be bounded at a_1. We show that by analyticity, this solution extends to $\overline{\mathbb{C}}\backslash[a_2, a_4]$. Next, we extend g to (a_2, a_4) by analytic continuation via the upper half plane to a_3^+ and require Re $g(x+i0)$ to be bounded at a_3. With this, we can define g as the function analytic on $\overline{\mathbb{C}}\backslash[a_2, a_4]$ and extended by Re $g(x + i0)$ on (a_2, a_4). Then, g satisfies the boundary conditions at a_1^+ and a_3^- and we prove that it also fulfills the transmission conditions (2.15), (2.16) at a_2 and hence is an eigenfunction of $\tilde{L}_S$. For large λ, the described procedure together with the local asymptotic behavior of solutions to $(L - \lambda)\phi = 0$ leads to finding the asymptotics of the eigenfunctions.

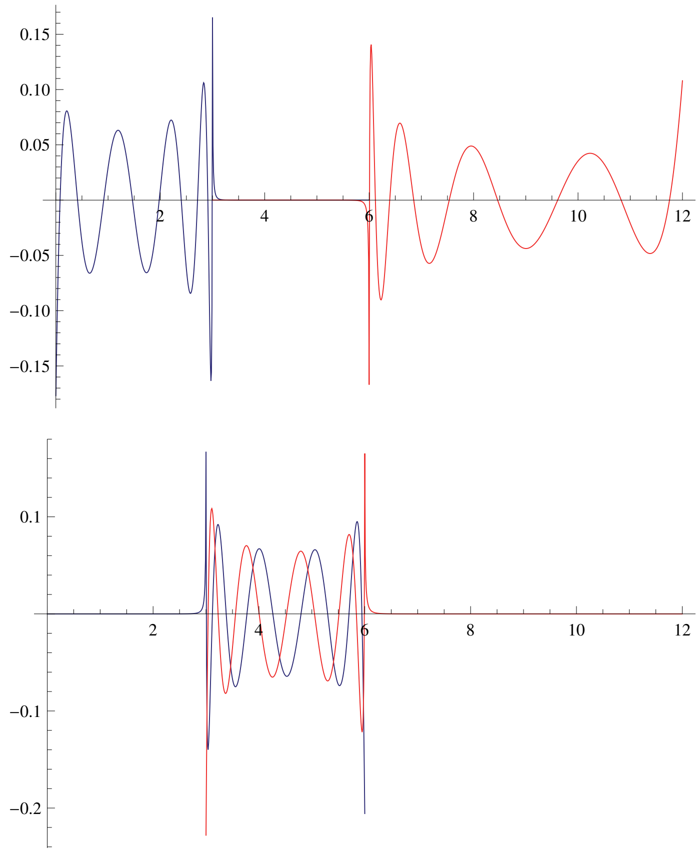

FIG. 1. *Examples of singular functions f_n (red) and g_n (blue) for $a_1 = 0, a_2 = 3, a_3 = 6$, $a_4 = 12$. Top: For σ_n close to 0, the singular functions are exponentially small on $[3, 6]$ and oscillate outside of $[3, 6]$. Bottom: For σ_n close to 1, the functions oscillate on $[3, 6]$ and are exponentially small outside of the overlap region.*

4.2. Validity of the approach. The solution $\phi = g$ to $(L-\lambda)\phi = 0$ is bounded at a_1 and therefore analytic on $\mathbb{C}\backslash[a_2, a_4]$. Furthermore, $g(z) = \mathcal{O}(1/z)$ as $z \to \infty$ and g is analytic at complex infinity (see [10]). We want to construct a solution g extended to (a_2, a_4) that also satisfies the transmission conditions at a_2 and the boundary condition at a_3. This transition at a_2 is not analytic (see [1]). In order to find the proper extension to (a_2, a_4), we will make explicit that g has to be the Hilbert transform of a function supported on $[a_2, a_4]$. To make use of this property, we first need to introduce the Riemann–Hilbert problem.

For a given function $f \in L^2(\gamma)$ on a simple smooth bounded oriented contour $\gamma \in \mathbb{C}$, find a function $F(z)$ such that

$$F(z) \text{ is analytic on } \overline{\mathbb{C}}\backslash\gamma, \tag{4.2}$$

$$F(z + i0) - F(z - i0) = 2if(z), \quad z \in \gamma, \tag{4.3}$$

$$F(z) \to 0 \text{ as } z \to \infty. \tag{4.4}$$

This Riemann–Hilbert problem is known to have the unique solution

$$F(z) = \frac{1}{\pi}\text{p.v.}\int_\gamma \frac{f(\tau)}{\tau - z}d\tau, \quad z \in \mathbb{C}. \tag{4.5}$$

(see [6, sections 14.2 and 16.3]). This statement can be used in a "reversed" sense: For any function F analytic on $\overline{\mathbb{C}}\backslash\gamma$ that satisfies (4.4), define the function f on γ to be

$$f(z) = \frac{F(z+i0) - F(z-i0)}{2i}, \quad z \in \gamma. \tag{4.6}$$

If $f \in L^2(\gamma)$, then by construction, F is the unique solution to the Riemann–Hilbert problem with right-hand side (4.6). Thus, $F(z) = 1/\pi$ p.v. $\int_\gamma f(\tau)/(\tau - z)d\tau$ on $\overline{\mathbb{C}}\backslash\gamma$.

Let $\gamma = [a_2, a_4]$, consider g on $\overline{\mathbb{C}}\backslash[a_2, a_4]$ from above, i.e., g is a solution to (4.1) and bounded at a_1, and define the function f on $[a_2, a_3) \cup (a_3, a_4]$ to be

$$f(x) := \frac{1}{2i}[g(x+i0) - g(x-i0)]. \tag{4.7}$$

Clearly, $f \in L^2([a_2, a_4])$ because g is analytic away from the points a_i and is either bounded or has a logarithmic singularity close to the points a_i. With that, $F = g$ is the only solution to the corresponding Riemann–Hilbert problem by uniqueness. Let $g_{2,4}$ denote the extension of g onto (a_2, a_4). With a slight abuse of notation, we will denote the function g extended by $g_{2,4}$ again by g. If we define $g_{2,4}(x) := \frac{1}{2}[g(x+i0) + g(x-i0)]$, the Plemelj–Sokhotksi formula yields that

$$g(x) \text{ extended by } g_{2,4}(x) \quad \text{on } (a_2, a_4) \tag{4.8}$$

is the Hilbert transform of $f(x)$ in (4.7), where f is supported on $[a_2, a_4]$. Note that both $f(x)$ and $g_{2,4}(x)$ are solutions to $(L - \lambda)\phi = 0$, because they are linear combinations of solutions.

For the construction of g in section 5, it will be useful to express $g_{2,4}$ by the analytic continuation of g via the upper half plane only, i.e., by $g(x + i0)$. This can be done as follows. Since $\lambda \in \mathbb{R}$, we can assume that g is real-valued on $\mathbb{R}\backslash[a_2, a_4]$. Hence, Im $Hf = 0$ on $\mathbb{R}\backslash[a_2, a_4]$ and thus, $f(x)$ is real-valued. Consequently, $g_{2,4}(x)$ is real-valued as well. If for two complex numbers a and b, $a + b \in \mathbb{R}$ and $a - b \in \mathbb{I}$, then Re a = Re b and Im a = −Im b. Thus,

$$g_{2,4}(x) = \text{Re } g(x + i0), \tag{4.9}$$
$$f(x) = \text{Im } g(x + i0). \tag{4.10}$$

With these relations, we can now show that $g(x)$ in (4.8) satisfies the transmission conditions (2.15), (2.16) at a_2.

With (2.13), (2.14), we can write g in a neighborhood of a_2^- as

$$g(x) = \sum_{n=0}^{\infty} d_n(x - a_2)^n + \ln|x - a_2| \sum_{n=0}^{\infty} b_n(x - a_2)^n, \quad x < a_2. \tag{4.11}$$

Since g is real-valued, $b_n, d_n \in \mathbb{R}$. The analytic continuation g_c of g from a_2^- to a_2^+ via the upper half plane is

$$g_c(x) = \sum_{n=0}^{\infty} d_n(x - a_2)^n + (\ln|x - a_2| - i\pi) \sum_{n=0}^{\infty} b_n(x - a_2)^n, \quad x > a_2. \tag{4.12}$$

By (4.8), (4.9), for x to the right of a_2, g is obtained by extracting the real part in (4.12). Comparing Re $g_c(x)$ with (4.11) then implies the transmission conditions (2.15) and (2.16) at a_2.

Remark 4.1. Another way to see that g extended by $g_{2,4}$ satisfies the transmission conditions is the following. The function f is a solution to $(L - \lambda)\phi = 0$ and thus is either bounded or of logarithmic singularity at a_2. Suppose f has a logarithmic singularity at a_2. Then, its Hilbert transform will have a singularity at a_2 that is stronger than logarithmic. This is a contradiction to $g = Hf$ being a solution to the differential equation $Lg = \lambda g$. Therefore, f has to be bounded at a_2. This implies that $g = Hf$ satisfies the transmission conditions at a_2.

The boundedness of $g_{2,4}$ at a_3 does not yet follow from the construction but rather has to be imposed explicitly. This is done by analytic continuation of g from the interior of (a_1, a_2) via the upper half plane to a neighborhood of a_3^+ and requiring Re $g(x + i0)$ to be bounded as $x \to a_3^+$. Using (2.13), (2.14), g to the right of a_3 can be represented by

$$g(x) = \text{Re}\left[\sum_{n=0}^{\infty} d_n(x-a_3)^n + \ln|x-a_3| \sum_{n=0}^{\infty} b_n(x-a_3)^n\right], \quad x > a_3,$$

with coefficients $b_n, d_n \in \mathbb{C}$. The requirement of boundedness then implies that the coefficient b_0 is purely imaginary. This together with using analytic continuation to express g to the left of a_3 by

$$g(x) = \text{Re}\left[\sum_{n=0}^{\infty} d_n(x-a_3)^n + (\ln|x-a_3| + i\pi) \sum_{n=0}^{\infty} b_n(x-a_3)^n\right], \quad x < a_3,$$

then yields that g is also bounded at a_3^-.

Thus, requiring boundedness of g at a_3^+ is sufficient to obtain that it is also bounded at a_3^-. This is useful because it allows for a procedure where the WKB approximation only needs to be matched to Bessel solutions on intervals where the solution is oscillatory, i.e., on (a_1, a_2) and (a_3, a_4). In these intervals, we can make use of the results from [10], where the asymptotics of the solutions to $(L - \lambda)\phi = 0$ close to the points a_i were obtained in the regions where the solutions oscillate.

5. Asymptotic analysis of the singular functions and singular values for $\boldsymbol{\sigma_n \to 0}$. In this section we want to make more precise the method motivated in the previous section. First, we need to introduce the WKB method.

As outlined in Remark 3.2, for $\lambda > 0$ large, the solution $\phi = g$ to $(L - \lambda)\phi = 0$ is oscillatory where P is negative, i.e., on $(a_1, a_2) \cup (a_3, a_4)$, and monotonic where P is positive. We approximate the solution g on (a_1, a_2) away from the endpoints by the WKB method. Then, we require that g be bounded at a_1. This is achieved by noting that local solutions of (4.1) close to the singular points a_i are approximated by linear combinations of Bessel functions of the first and second kind, [10] (we will refer to solutions of this type as Bessel solutions). Since the second kind Bessel function is singular at the origin, we match g with a local solution at a_1^+, which is approximated by a Bessel function of the first kind. The next step is to analytically continue the WKB approximation via the upper half plane to the region to the right of a_3. This will be an approximation to the solution g in that region because the WKB approximation is valid with a uniform accuracy (see [10]). Recall that on (a_2, a_4), g is defined as $g_{2,4}(x) = \text{Re } g(x + i0)$. At a_3^+, we require boundedness of Re $g(x + i0)$ by matching it with a Bessel solution of which the coefficient in front of the unbounded part is purely imaginary (see Figure 2 for a sketch of this procedure). As will be seen, this requirement leaves us with a discrete set $\{\lambda_n\}_{n\in\mathbb{N}}$ for which $L_S g_n = \lambda_n g_n$, $\lambda_n \to +\infty$.

In what follows we will use the following two quantities:

$$K_- := \int_{a_1}^{a_2} \frac{1}{\sqrt{-P(x)}} dx, \; K_+ := \int_{a_2}^{a_3} \frac{1}{\sqrt{P(x)}} dx.$$

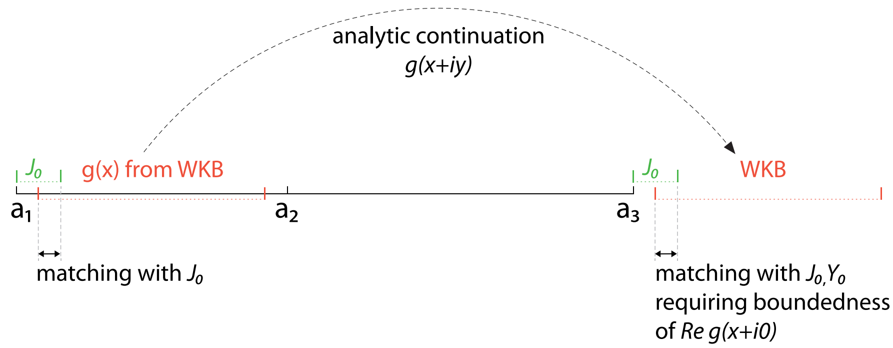

FIG. 2. *Sketch of the construction of the g_n's from WKB and Bessel approximations.*

One can show that also

$$K_- = \int_{a_3}^{a_4} \frac{1}{\sqrt{-P(x)}} dx$$

holds (see [10]).

5.1. The WKB approximation and its region of validity. We consider the WKB method in order to obtain approximations for solutions g to $Lg = \lambda g$ and large λ on the interior of the intervals where the solutions oscillate, i.e., on $[a_1 + \delta, a_2 - \delta]$ and $[a_3 + \delta, a_4 - \delta]$ (for some small δ to be defined). We start by considering a solution on $[a_1 + \delta, a_2 - \delta]$ and define $\epsilon := 1/\sqrt{\lambda}$. Let C_0^+ be the upper half of the complex plane including the real line, and let a^- and $a_{3,4}^*$ be arbitrary but fixed real numbers such that $a^- < a_1$ and $a_{3,4}^* \in (a_3, a_4)$. It has been shown in [10] that for a sufficiently small $\mu_1 > 0$ a connected region $\Lambda_- \subset C_0^+$ exists, such that Λ_- contains the segment $[a^-, a_{3,4}^*]$, except for $\mathcal{O}(\epsilon^{2(1-\mu_1)})$ size neighborhoods of a_1, a_2, a_3, and such that the following holds.

THEOREM 5.1 (Theorem B.3 in [10]). *Using the WKB method, for every sufficiently small $\mu_1 > 0$ independent of ϵ, the solutions of $(L - \lambda)\phi = 0$ are linear combinations of*

$$\hat{\phi}_1(z) = \frac{1}{P(z)^{1/4}} e^{\sqrt{\lambda}\int_a^z \frac{d\xi}{\sqrt{P(\xi)}}} (1 + \mathcal{O}(\epsilon^{\mu_1})), \tag{5.1}$$

$$\hat{\phi}_2(z) = \frac{1}{P(z)^{1/4}} e^{-\sqrt{\lambda}\int_a^z \frac{d\xi}{\sqrt{P(\xi)}}} (1 + \mathcal{O}(\epsilon^{\mu_1})), \tag{5.2}$$

where the accuracy $\mathcal{O}(\epsilon^{\mu_1})$ is uniform in the region Λ_-. The point a can, for example, be chosen to be $a_1, a_2,$ or a_3.

The same holds in a region $\Lambda_+ \subset C_0^+$ which contains the segment $[a_{1,2}^*, a^+]$ except for $\mathcal{O}(\epsilon^{2(1-\mu_1)})$ size neighborhoods of a_2, a_3, a_4. Here, a^+ and $a_{1,2}^*$ are arbitrary but fixed numbers such that $a^+ > a_4$ and $a_{1,2}^* \in (a_1, a_2)$; see [10]. Figure 3 shows a sketch of the two regions Λ_- and Λ_+.

5.2. The Bessel solutions and their region of validity. For $x \in (a_1, a_2) \cup (a_3, a_4)$ define $t = -\lambda(x - a_i)/P'(a_i)$ for fixed $i = 1, \ldots, 4$ and let μ_2 be a small positive parameter independent of λ.

Then, the two linearly independent solutions to $(L - \lambda)\phi = 0$ in a region $x - a_i = \mathcal{O}(\epsilon^{2\mu_2})$ for $t \in [0, 1)$ can be written as

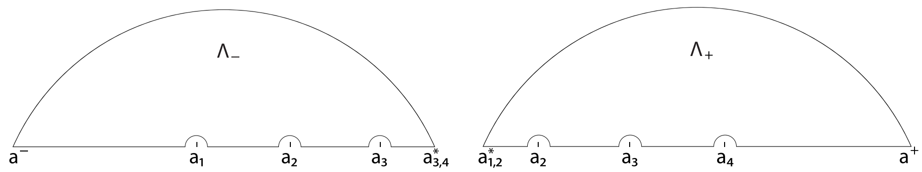

FIG. 3. *Sketches of the regions* Λ_- *and* Λ_+ *on which the WKB approximations are valid with uniform accuracy.*

$$\hat{\psi}_1(x-a_i) = J_0(2\sqrt{t}) + \mathcal{O}(t/\lambda) = J_0(2\sqrt{t}) + \mathcal{O}(\epsilon^{2\mu_2}), \tag{5.3}$$

$$\hat{\psi}_2(x-a_i) = Y_0(2\sqrt{t}) + \mathcal{O}(t^{1/2}/\lambda) = Y_0(2\sqrt{t}) + \mathcal{O}(\epsilon^{1+\mu_2}) \tag{5.4}$$

and for $t \in [1, \mathcal{O}(\epsilon^{2(\mu_2-1)})]$ as

$$\hat{\psi}_1(x-a_i) = J_0(2\sqrt{t}) + t^{-1/4}\mathcal{O}(\epsilon^{2\mu_2}), \tag{5.5}$$

$$\hat{\psi}_2(x-a_i) = Y_0(2\sqrt{t}) + t^{-1/4}\mathcal{O}(\epsilon^{2\mu_2}), \tag{5.6}$$

where J_0 and Y_0 denote the Bessel functions of the first and the second kind, respectively [10].

LEMMA 5.2 (properties of J_0 and Y_0). *The following holds for small arguments* $0 < z \ll 1$*:*

$$J_0(z) = 1 + \mathcal{O}(z^2), \tag{5.7}$$

$$Y_0(z) = \frac{2}{\pi}\left[\ln\left(\frac{z}{2}\right) + \gamma\right] + \mathcal{O}(z^2 \ln z), \tag{5.8}$$

where γ *denotes the Euler–Mascheroni constant. The asymptotic behavior for arguments* $z \to +\infty$ *is*

$$J_0(z) = \sqrt{\frac{2}{\pi z}}\left[\cos\left(z - \frac{\pi}{4}\right) + \mathcal{O}(1/z)\right], \tag{5.9}$$

$$Y_0(z) = \sqrt{\frac{2}{\pi z}}\left[\sin\left(z - \frac{\pi}{4}\right) + \mathcal{O}(1/z)\right]. \tag{5.10}$$

5.3. Overlap region of validities. If $1 - \mu_1 > \mu_2$ and $x \in (a_1, a_2) \cup (a_3, a_{3,4}^*)$, both the WKB solutions (5.1), (5.2), with accuracy $\mathcal{O}(\epsilon^{\mu_1})$, and the Bessel solutions (5.5), (5.6), with accuracy $\mathcal{O}(\epsilon^{2\mu_2})$, are valid in the region

$$C_1\epsilon^{2(1-\mu_1)} < |x - a_i| < C_2\epsilon^{2\mu_2} \tag{5.11}$$

for positive constants C_1, C_2 and $i = 1, 2, 3$ (Corollary B.11, in [10]). This also holds for $x \in (a_{1,2}^*, a_2) \cup (a_3, a_4)$ and $i = 2, 3, 4$.

5.4. Derivation of the asymptotics.

5.4.1. The WKB approximation in (a_1, a_2) away from the endpoints. Using (5.1) and (5.2) with $a = a_1$, the WKB solution to $Lg = \lambda g$ is

$$g(x) = \frac{1}{(-P(x))^{1/4}} \left[\cos\left(\frac{1}{\epsilon} \int_{a_1}^{x} \frac{dt}{\sqrt{-P(t)}} - \frac{\pi}{4} \right) \cdot (1 + \mathcal{O}(\epsilon^{\mu_1})) + c_1 \sin\left(\frac{1}{\epsilon} \int_{a_1}^{x} \frac{dt}{\sqrt{-P(t)}} - \frac{\pi}{4} \right) \cdot (1 + \mathcal{O}(\epsilon^{\mu_1})) \right] \tag{5.12}$$

for a constant c_1 and it is valid on $x \in [a_1 + \mathcal{O}(\epsilon^{2(1-\mu_1)}), a_2 - \mathcal{O}(\epsilon^{2(1-\mu_1)})]$. Here we have assumed without loss of generality that the constant in front of the term involving cosine is equal to 1.

5.4.2. Bounded Bessel solution at a_1^+. Let $\hat{\psi}_1(x)$ and $\hat{\psi}_2(x)$ denote the two linearly independent solutions in the region $x - a_1 = \mathcal{O}(\epsilon^{2\mu_2})$. The boundedness of g in this region requires that for $t = \lambda(a_1 - x)/P'(a_1)$, $t \in [0, 1)$, and constants b_1 and b_2 in

$$g(x) = b_1 \cdot \hat{\psi}_1(x - a_1) + b_2 \cdot \hat{\psi}_2(x - a_1), \tag{5.13}$$

the coefficient b_2 be equal to zero. Thus, for $t \in [1, \mathcal{O}(\epsilon^{2(\mu_2 - 1)})]$

$$g(x) = b_1 \cdot [J_0(2\sqrt{t}) + t^{-1/4}\mathcal{O}(\epsilon^{2\mu_2})]. \tag{5.14}$$

The two solutions (5.12), (5.14) need to be matched in the overlap region in which they are both valid, i.e., for x such that

$$\mathcal{O}(\epsilon^{2(1-\mu_1)}) \leq x - a_1 \leq \mathcal{O}(\epsilon^{2\mu_2}). \tag{5.15}$$

For this, we approximate the first factor in (5.12) by:

$$\frac{1}{(-P(x))^{1/4}} = \frac{1 + \mathcal{O}(x - a_1)}{((a_1 - x)P'(a_1))^{1/4}}, \tag{5.16}$$

and for the arguments in the trigonometric expressions we can write

$$\begin{aligned} \int_{a_1}^{x} \frac{dt}{\sqrt{-P(t)}} &= \int_{a_1}^{x} \frac{1 + \mathcal{O}(t - a_1)}{\sqrt{P'(a_1)(a_1 - t)}} dt \\ &= \frac{1}{(-P'(a_1))^{1/2}} \int_{a_1}^{x} \frac{dt}{\sqrt{t - a_1}} + \int_{a_1}^{x} \mathcal{O}\left((t - a_1)^{1/2} \right) dt \\ &= 2\sqrt{\frac{a_1 - x}{P'(a_1)}} + \mathcal{O}((x - a_1)^{3/2}). \end{aligned} \tag{5.17}$$

Taylor expansions of the cosine and sine functions then results in

$$\cos\left(\frac{1}{\epsilon} \int_{a_1}^{x} \frac{dt}{\sqrt{-P(t)}} - \frac{\pi}{4} \right) = \cos\left(\frac{2}{\epsilon} \sqrt{\frac{a_1 - x}{P'(a_1)}} - \frac{\pi}{4} \right) + \mathcal{O}((x - a_1)^{3/2}/\epsilon), \tag{5.18}$$

$$\sin\left(\frac{1}{\epsilon} \int_{a_1}^{x} \frac{dt}{\sqrt{-P(t)}} - \frac{\pi}{4} \right) = \sin\left(\frac{2}{\epsilon} \sqrt{\frac{a_1 - x}{P'(a_1)}} - \frac{\pi}{4} \right) + \mathcal{O}((x - a_1)^{3/2}/\epsilon). \tag{5.19}$$

Since $x - a_1$ lies in the overlap region (5.15), the following holds:

$$\mathcal{O}((x-a_1)^{3/2}/\epsilon) = \mathcal{O}(\epsilon^{3\mu_2 - 1}). \tag{5.20}$$

Inserting (5.20) in (5.18) and (5.19), we obtain for the WKB solution in the overlap region of validity

$$\begin{aligned} g(x) &= \frac{1+\mathcal{O}(x-a_1)}{((a_1-x)P'(a_1))^{1/4}} \cdot \Bigg[\cos\Bigg(\frac{2}{\epsilon}\sqrt{\frac{a_1-x}{P'(a_1)}} - \frac{\pi}{4}\Bigg) \\ &\quad + c_1 \sin\Bigg(\frac{2}{\epsilon}\sqrt{\frac{a_1-x}{P'(a_1)}} - \frac{\pi}{4}\Bigg) + \mathcal{O}(\epsilon^{\min\{\mu_1, 3\mu_2-1\}})\Bigg] \\ &= \frac{1}{((a_1-x)P'(a_1))^{1/4}} \cdot \Bigg[\cos\Bigg(\frac{2}{\epsilon}\sqrt{\frac{a_1-x}{P'(a_1)}} - \frac{\pi}{4}\Bigg) \\ &\quad + c_1 \sin\Bigg(\frac{2}{\epsilon}\sqrt{\frac{a_1-x}{P'(a_1)}} - \frac{\pi}{4}\Bigg) + \mathcal{O}(\epsilon^{\min\{\mu_1, 3\mu_2-1, 2\mu_2\}})\Bigg]. \end{aligned} \tag{5.21}$$

We now select μ_1 and μ_2 such that the error term in the last equation tends to zero and such that $1 - \mu_1 > \mu_2$. A convenient choice is

$$\mu_1 = \frac{1}{2} - \delta, \quad \mu_2 = \frac{1}{2} - \frac{\delta}{3} \tag{5.22}$$

for a small fixed $\delta > 0$, as done in [10]. The WKB solution has to be matched with the Bessel solution in (5.14) in the overlap region (5.15). We do this by matching the two solutions for large $t = \lambda(a_1 - x)/P'(a_1)$ and exploiting the asymptotics (5.9) of the Bessel function J_0, which gives

$$g(x) = b_1\sqrt{\epsilon}\left(\frac{P'(a_1)}{a_1-x}\right)^{1/4}\left[\frac{1}{\sqrt{\pi}}\cos\left(\frac{2}{\epsilon}\sqrt{\frac{a_1-x}{P'(a_1)}} - \frac{\pi}{4}\right) + \mathcal{O}\left(\frac{\epsilon}{\sqrt{x-a_1}}\right) + \mathcal{O}\left(\epsilon^{1-2\delta/3}\right)\right].$$

From $(x-a_1)^{-1/2} = \mathcal{O}\left(\epsilon^{-(\delta+1/2)}\right)$, we conclude

$$g(x) = b_1\sqrt{\epsilon}\left(\frac{P'(a_1)}{a_1-x}\right)^{1/4}\left[\frac{1}{\sqrt{\pi}}\cos\left(\frac{2}{\epsilon}\sqrt{\frac{a_1-x}{P'(a_1)}} - \frac{\pi}{4}\right) + \mathcal{O}\left(\epsilon^{1/2-\delta}\right)\right]. \tag{5.23}$$

Matching the two solutions (5.21) and (5.23) determines the constants b_1 and c_1:

$$b_1 = \sqrt{\frac{\pi}{-\epsilon P'(a_1)}}\left(1 + \mathcal{O}(\epsilon^{1/2-\delta})\right), \tag{5.24}$$

$$c_1 = \mathcal{O}(\epsilon^{1/2-\delta}). \tag{5.25}$$

Thus, the solution g is of the form

$$\begin{aligned} g(x) = \frac{1}{(-P(x))^{1/4}} &\Bigg[\cos\Bigg(\frac{1}{\epsilon}\int_{a_1}^{x}\frac{dt}{\sqrt{-P(t)}} - \frac{\pi}{4}\Bigg) \cdot (1 + \mathcal{O}(\epsilon^{1/2-\delta})) \\ &+ \mathcal{O}(\epsilon^{1/2-\delta})\sin\Bigg(\frac{1}{\epsilon}\int_{a_1}^{x}\frac{dt}{\sqrt{-P(t)}} - \frac{\pi}{4}\Bigg)\Bigg] \end{aligned} \tag{5.26}$$

on the interval $x \in [a_1 + \mathcal{O}(\epsilon^{1+2\delta}), a_2 - \mathcal{O}(\epsilon^{1+2\delta})]$.

5.4.3. Analytic continuation to a_3^+. The next step consists of analytically continuing g in (5.26) to a_3^+ via the upper half plane. Since the WKB approximation is valid in Λ_- with uniform accuracy $\mathcal{O}(\epsilon^{1/2-\delta})$ (Theorem 5.1), the analytic continuation of the WKB approximation (5.26) is an approximation to the analytic continuation of g. Taking into account the phase shifts of P and using

$$\int_{a_1}^{x} \frac{dt}{\sqrt{-P(t)}} = \int_{a_1}^{a_2} \frac{dt}{\sqrt{-P(t)}} + i\int_{a_2}^{a_3} \frac{dt}{\sqrt{P(t)}} - \int_{a_3}^{x} \frac{dt}{\sqrt{-P(t)}} = K_- + iK_+ - \int_{a_3}^{x} \frac{dt}{\sqrt{-P(t)}}, \tag{5.27}$$

we obtain

$$\begin{aligned} g(x+i0) &= \frac{i}{(-P(x))^{1/4}} \cdot \Bigg[\cos\left(\frac{1}{\epsilon}\int_{a_3}^{x} \frac{dt}{\sqrt{-P(t)}} - \frac{K_-}{\epsilon} - i\frac{K_+}{\epsilon} + \frac{\pi}{4}\right) \cdot \left(1 + \mathcal{O}(\epsilon^{1/2-\delta})\right) \\ &\qquad - \sin\left(\frac{1}{\epsilon}\int_{a_3}^{x} \frac{dt}{\sqrt{-P(t)}} - \frac{K_-}{\epsilon} - i\frac{K_+}{\epsilon} + \frac{\pi}{4}\right) \cdot \mathcal{O}(\epsilon^{1/2-\delta})\Bigg], \end{aligned}$$

where $x \in [a_3 + \mathcal{O}(\epsilon^{1+2\delta}), a_{3,4}^*]$. The properties of the complex valued trigonometric functions yield

$$\begin{aligned} g(x+i0) = \frac{i}{(-P(x))^{1/4}} \cdot \Bigg[&\Bigg\{\cos\left(\frac{1}{\epsilon}\int_{a_3}^{x} \frac{dt}{\sqrt{-P(t)}} - \frac{K_-}{\epsilon} + \frac{\pi}{4}\right) \cdot \cosh\left(-\frac{K_+}{\epsilon}\right) \\ &- i\sin\left(\frac{1}{\epsilon}\int_{a_3}^{x} \frac{dt}{\sqrt{-P(t)}} - \frac{K_-}{\epsilon} + \frac{\pi}{4}\right) \cdot \sinh\left(-\frac{K_+}{\epsilon}\right)\Bigg\} \cdot \left(1 + \mathcal{O}(\epsilon^{1/2-\delta})\right) \\ &+\mathcal{O}\left(\epsilon^{1/2-\delta}\right) \cdot \Bigg\{\sin\left(\frac{1}{\epsilon}\int_{a_3}^{x} \frac{dt}{\sqrt{-P(t)}} - \frac{K_-}{\epsilon} + \frac{\pi}{4}\right) \cdot \cosh\left(-\frac{K_+}{\epsilon}\right) \\ &+ i\cos\left(\frac{1}{\epsilon}\int_{a_3}^{x} \frac{dt}{\sqrt{-P(t)}} - \frac{K_-}{\epsilon} + \frac{\pi}{4}\right) \cdot \sinh\left(-\frac{K_+}{\epsilon}\right)\Bigg\}\Bigg]. \end{aligned}$$

So far, g is a function that is not normalized on $[a_1, a_3]$. However, we will need to work with singular functions that have their L^2-norm equal to 1 on $[a_1, a_3]$ in order to estimate the singular values correctly. Thus, we incorporate $\|g\|_{L^2([a_1,a_3])}$ derived in (8.1) in the appendix, simplify the above expression, and use the relation $\sin x = \cos(x - \frac{\pi}{2})$ to obtain a new normalized function g:

$$\begin{aligned} g(x+i0) = \sqrt{\frac{2}{K_-}} \frac{-e^{K_+/\epsilon}}{2(-P(x))^{1/4}} \cdot \Bigg[&\cos\left(\frac{1}{\epsilon}\int_{a_3}^{x} \frac{dt}{\sqrt{-P(t)}} - \frac{K_-}{\epsilon} - \frac{\pi}{4}\right) \\ &+ i\sin\left(\frac{1}{\epsilon}\int_{a_3}^{x} \frac{dt}{\sqrt{-P(t)}} - \frac{K_-}{\epsilon} - \frac{\pi}{4}\right) + \mathcal{O}\left(\epsilon^{1/2-\delta}\right)\Bigg]. \end{aligned} \tag{5.28}$$

Next, we match this solution to a linear combination of Bessel approximations at a_3^+ and then require boundedness of its real part.

In the overlap region (5.11) close to a_3^+ where both WKB and Bessel solutions are valid, we define $t = \lambda(a_3 - x)/P'(a_3)$. The function P in (5.28) can be approximated in the same way as at a_1^+ in (5.16)–(5.19). Factorizing the trigonometric expression, the WKB solution (5.28) can then be written as

$$g(x+i0) = -\sqrt{\frac{1}{2K_-}}\frac{e^{K_+/\epsilon}}{((a_3-x)P'(a_3))^{1/4}}e^{-iK_-/\epsilon}\cdot\left[\cos\left(\frac{2}{\epsilon}\sqrt{\frac{a_3-x}{P'(a_3)}}-\frac{\pi}{4}\right)\right. \\ \left.+\, i\sin\left(\frac{2}{\epsilon}\sqrt{\frac{a_3-x}{P'(a_3)}}-\frac{\pi}{4}\right)+\mathcal{O}(\epsilon^{1/2-\delta})\right]. \tag{5.29}$$

In the overlap region (5.11) the Bessel solution is a linear combination of the solution $\hat{\psi}_1$ in (5.5) bounded at a_3^+ and the solution $\hat{\psi}_2$ in (5.6) having a singularity at a_3^+,

$$g(x) = b_3\hat{\psi}_1(x-a_3)+c_3\hat{\psi}_2(x-a_3) \tag{5.30}$$

for constants b_3 and c_3. To ensure boundedness at a_3^+ of the real part of (5.30), we will need to impose Re $c_3 = 0$. The asymptotics of J_0 and Y_0 in (5.9) and (5.10) for large t allow us to write the Bessel solution similarly to (5.23) but with an additional term in Y_0:

$$g(x) = \sqrt{\frac{\epsilon}{\pi}}\left(\frac{P'(a_3)}{a_3-x}\right)^{1/4}\left(b_3\left[\cos\left(\frac{2}{\epsilon}\sqrt{\frac{a_3-x}{P'(a_3)}}-\frac{\pi}{4}\right)+\mathcal{O}(\epsilon^{1/2-\delta})\right]\right. \\ \left.+\,c_3\left[\sin\left(\frac{2}{\epsilon}\sqrt{\frac{a_3-x}{P'(a_3)}}-\frac{\pi}{4}\right)+\mathcal{O}(\epsilon^{1/2-\delta})\right]\right). \tag{5.31}$$

From the matching of (5.29) with (5.31) for large t, we obtain

$$b_3 = -ic_3(1+\mathcal{O}(\epsilon^{1/2-\delta})). \tag{5.32}$$

The requirement Re $c_3 = 0$ then implies Im $b_3 =$ Im $c_3\cdot\mathcal{O}(\epsilon^{1/2-\delta})$ and hence

$$b_3 = \text{Re } b_3\cdot(1+\mathcal{O}(\epsilon^{1/2-\delta})) \tag{5.33}$$

or more explicitly

$$b_3 = -\sqrt{\frac{\pi}{2K_-\epsilon}}\frac{e^{K_+/\epsilon}}{\sqrt{-P'(a_3)}}\cos\left(\frac{K_-}{\epsilon}\right)(1+\mathcal{O}(\epsilon^{1/2-\delta})). \tag{5.34}$$

The matching also yields that Re $c_3 = 0$ implies Re $(ie^{-iK_-/\epsilon}) = \mathcal{O}(\epsilon^{1/2-\delta})$. Thus,

$$\sin\left(\frac{K_-}{\epsilon}\right) = \mathcal{O}(\epsilon^{1/2-\delta}) \tag{5.35}$$

and as a result

$$\frac{K_-}{\epsilon} = n\pi + \mathcal{O}\big(\epsilon^{1/2-\delta}\big) \tag{5.36}$$

for $n\in\mathbb{N}$. This equation for the parameter $\epsilon = 1/\sqrt{\lambda}$, where λ is a large positive eigenvalue of the operator L_S, shows the essential property of the spectrum of L_S to be purely discrete and, in addition, reveals the rate at which the eigenvalues tend to $+\infty$. Since the spectrum of L_S is unbounded both above and below, we have to make a choice in terms of the enumeration of the eigenvalues λ_n. Equation (5.36) shows that we can choose the enumeration such that

$$\sqrt{\lambda_n} = \frac{n\pi}{K_-} + \mathcal{O}\big(n^{-1/2+\delta}\big), \quad n \in \mathbb{N}, \tag{5.37}$$

holds. With this and (5.34) we finally obtain the coefficient b_3:

$$b_3 = (-1)^{n+1}\sqrt{\frac{\pi}{2K_-\epsilon}}\frac{e^{K_+/\epsilon}}{\sqrt{-P'(a_3)}}(1+\mathcal{O}(\epsilon^{1/2-\delta})). \tag{5.38}$$

5.5. Asymptotic behavior of the singular values accumulating at zero. In the previous sections we have obtained the asymptotics of the functions g with $\|g\|_{L^2([a_1,a_3])} = 1$ and the property that $\chi_{[a_1,a_3]}g$ are the singular functions of H_T for singular values close to zero. We found g by defining it to be equal to the analytic function on $\bar{\mathbb{C}}\backslash[a_2,a_4]$ extended by $g_{2,4}$ on (a_2,a_4); see (4.8). These functions g are the Hilbert transforms of functions f that are supported on $[a_2,a_4]$. If we normalize f as well, this reads $Hf = \sigma g$, where $\sigma \ll 1$ is the corresponding singular value of H_T. Applying the Hilbert transform on both sides gives $Hg = -\frac{1}{\sigma}f$. Thus, in order to estimate σ, we can proceed as follows:

1. Estimate the jump discontinuity $g(a_3^+) - g(a_3^-)$.
2. Find the logarithmic term in $(Hg)(a_3^+)$.
3. Determine the logarithmic term in $f(a_3^+)$.
4. Estimate $\sigma = -f(a_3^+)/(Hg)(a_3^+)$.

Combining the asymptotics of the Bessel solutions (5.3), (5.4) with the representation (5.30) of g close to a_3^+ yields the following asymptotics for g:

$$g(x) = b_3 \cdot \big[J_0(2\sqrt{t}) + \mathcal{O}(\epsilon^{1-2\delta/3})\big] + c_3 \cdot \big[Y_0(2\sqrt{t}) + \mathcal{O}(\epsilon^{3/2-\delta/3})\big],$$

where $t = \lambda(a_3 - x)/P'(a_3) \in [0,1)$. Using the relation (5.32) between b_3 and c_3, we can further write this as

$$g(x) = -ic_3 \cdot \big[J_0(2\sqrt{t}) + \mathcal{O}(\epsilon^{1/2-\delta})\big] + c_3 \cdot \big[Y_0(2\sqrt{t}) + \mathcal{O}(\epsilon^{3/2-\delta/3})\big].$$

On the other hand, we know from the theory of Fuchs and Frobenius that close to a_3^+ a solution to $(L-\lambda)g = 0$ is of the form

$$g(x) = \phi_1(x) + \phi_2(x)\ln|x-a_3|,$$

where ϕ_1, ϕ_2 are analytic close to a_3. The requirement that Re $g(a_3^+)$ be bounded implies Re $\phi_2(a_3) = 0$. The analytic continuation of g to a neighborhood of a_3^- is given by

$$g_c(x) = \phi_1(x) + \phi_2(x)[\ln|x-a_3| + i\pi].$$

According to (4.9), g at a_3^- is equal to Re $g_c(x)$. This determines the jump discontinuity of g across a_3 to be $-i\pi\phi_2(a_3)$. Hence, using the asymptotics (5.8) of Y_0, the jump discontinuity of g at a_3 is equal to

$$g(a_3^+) - g(a_3^-) = -i\pi\phi_2(a_3) = -ic_3 = b_3(1+\mathcal{O}(\epsilon^{1/2-\delta})).$$

This allows us to estimate the logarithmic term in Hg to be

$$-\frac{1}{\pi}b_3(1+\mathcal{O}(\epsilon^{1/2-\delta}))\ln|x-a_3|$$

(see section 8.2 in [6]).

Next, we find f such that supp $f = [a_2, a_4]$ and $Lf = \lambda f$ with a WKB approximation which holds on the region Λ_+. On (a_3, a_4), f is oscillatory, so analogously to the procedure for g, we start with the WKB approximation on $[a_3 + \mathcal{O}(\epsilon^{1+2\delta}), a_4 - \mathcal{O}(\epsilon^{1+2\delta})]$ and require boundedness at a_4^+. This determines f (similarly to (5.26) for g) up to a constant:

$$f(x) = \frac{1}{(-P(x))^{1/4}} \left[\cos\left(\frac{1}{\epsilon} \int_x^{a_4} \frac{dt}{\sqrt{-P(t)}} - \frac{\pi}{4} \right) \cdot (1 + \mathcal{O}(\epsilon^{1/2-\delta})) + \sin\left(\frac{1}{\epsilon} \int_x^{a_4} \frac{dt}{\sqrt{-P(t)}} - \frac{\pi}{4} \right) \cdot \mathcal{O}(\epsilon^{1/2-\delta}) \right].$$

Before, we estimated g at a_3^+ and required its real part to be bounded. Now, in the procedure for f, we are interested in estimating the *unbounded* part of f at a_3^+. We make use of the relation

$$\int_{a_3}^{x} \frac{dt}{\sqrt{-P(t)}} = \int_{a_3}^{a_4} \frac{dt}{\sqrt{-P(t)}} + \int_{a_4}^{x} \frac{dt}{\sqrt{-P(t)}} = -\int_{x}^{a_4} \frac{dt}{\sqrt{-P(t)}} + K_-,$$

which allows us to rewrite f on $[a_3 + \mathcal{O}(\epsilon^{1+2\delta}), a_4 - \mathcal{O}(\epsilon^{1+2\delta})]$:

$$f(x) = \frac{1}{(-P(x))^{1/4}} \left[\cos\left(-\frac{1}{\epsilon} \int_{a_3}^{x} \frac{dt}{\sqrt{-P(t)}} + \frac{K_-}{\epsilon} - \frac{\pi}{4} \right) \cdot (1 + \mathcal{O}(\epsilon^{1/2-\delta})) + \mathcal{O}(\epsilon^{1/2-\delta}) \sin\left(-\frac{1}{\epsilon} \int_{a_3}^{x} \frac{dt}{\sqrt{-P(t)}} + \frac{K_-}{\epsilon} - \frac{\pi}{4} \right) \right]. \tag{5.39}$$

Using (5.36) and trigonometric identities, it then follows that

$$f(x) = \frac{(-1)^n}{(-P(x))^{1/4}} \left[-\sin\left(\frac{1}{\epsilon} \int_{a_3}^{x} \frac{dt}{\sqrt{-P(t)}} - \frac{\pi}{4} \right) + \mathcal{O}(\epsilon^{1/2-\delta}) - \cos\left(\frac{1}{\epsilon} \int_{a_3}^{x} \frac{dt}{\sqrt{-P(t)}} - \frac{\pi}{4} \right) \cdot \mathcal{O}(\epsilon^{1/2-\delta}) \right] \tag{5.40}$$

on $[a_3 + \mathcal{O}(\epsilon^{1+2\delta}), a_4 - \mathcal{O}(\epsilon^{1+2\delta})]$.

In a neighborhood of a_3^+, f can be represented as a linear combination of the Bessel solutions (5.5) and (5.6). For constants b_3', c_3',

$$f(x) = b_3' \left[J_0(2\sqrt{t}) + t^{-1/4} \mathcal{O}(\epsilon^{1-2\delta/3}) \right] + c_3' \left[Y_0(2\sqrt{t}) + t^{-1/4} \mathcal{O}(\epsilon^{1-2\delta/3}) \right], \tag{5.41}$$

where $t = \lambda(a_3 - x)/P'(a_3)$ and $t \in [1, \mathcal{O}(\epsilon^{-1-2\delta/3})]$. Using the asymptotics of the Bessel functions for $t \to +\infty$ (5.5), (5.6) to match the above with the WKB solution (5.40) in their overlap region of validity (similarly as in section 5.4.2) results in

$$b_3' = (-1)^{n+1} \sqrt{\frac{\pi}{-\epsilon P'(a_3)}} \cdot \mathcal{O}(\epsilon^{1/2-\delta}), \tag{5.42}$$

$$c_3' = (-1)^{n+1} \sqrt{\frac{\pi}{-\epsilon P'(a_3)}} \cdot (1 + \mathcal{O}(\epsilon^{1/2-\delta})). \tag{5.43}$$

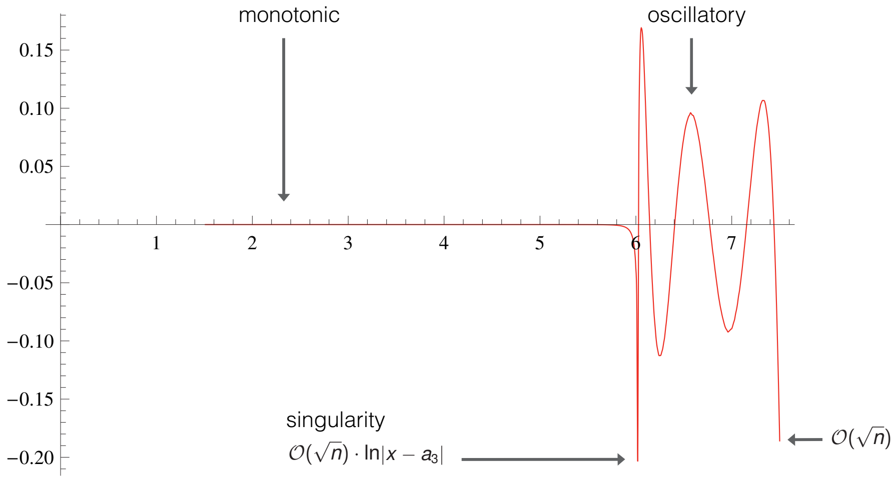

FIG. 4. *The asymptotic behavior of the singular functions f_n as $\sigma_n \to 0$ for $a_1 = 0, a_2 = 1.5, a_3 = 6, a_4 = 7.5$. The behavior at a_3 is obtained from* (5.44) *and the behavior at a_4 is analogous to that of g_n at a_1 (see section* 5.4.2*).*

After normalization of f (as was done for g; see the appendix), we can find the logarithmic term in $f(a_3^+)$ (up to a sign) with the help of (5.8),

$$\frac{(-1)^{n+1}}{\pi}\sqrt{\frac{2\pi}{-\epsilon P'(a_3)K_-}}\ln|x-a_3|(1+\mathcal{O}(\epsilon^{1/2-\delta})); \tag{5.44}$$

see Figure 4. The sign of f is then determined by $f = -\sigma Hg$ and $\sigma > 0$. This yields

$$\begin{aligned}(Hg)(a_3^+)/f(a_3^+) &= \frac{\frac{(-1)^n}{\pi}\sqrt{\frac{\pi}{2K_-\epsilon}}\frac{e^{K_+/\epsilon}}{\sqrt{-P'(a_3)}}}{(-1)^{n+1}\sqrt{\frac{2\pi}{-\epsilon P'(a_3)K_-}}\cdot\frac{1}{\pi}}\cdot(1+\mathcal{O}(\epsilon^{1/2-\delta}))\\ &= -\frac{1}{2}e^{K_+/\epsilon}(1+\mathcal{O}(\epsilon^{1/2-\delta}))\end{aligned}$$

and

$$\sigma = 2e^{-K_+/\epsilon}(1+\mathcal{O}(\epsilon^{1/2-\delta})). \tag{5.45}$$

THEOREM 5.3. *Let λ_n be enumerated as in* (5.37)*. Then, the singular values σ_n of H_T that accumulate at zero behave asymptotically like*

$$\sigma_n = 2e^{-n\pi K_+/K_-}(1+\mathcal{O}(n^{-1/2+\delta})),\ n\to\infty. \tag{5.46}$$

This is the main result of our paper. It shows the *severe* ill-posedness of the underlying problem of reconstructing a function f from $H_T\Phi = \Psi$ for given Ψ: A subsequence of the singular values σ_n of H_T decays to zero, resulting in the unboundedness of the inverse of H_T. As a consequence, small perturbations in Ψ due to measurement noise will result in unreliable predictions for Φ. Unlike in cases of so-called mild ill-posedness, where the singular values decay to zero at a polynomial rate, the singular values σ_n of H_T decay to zero exponentially, resulting in severe ill-posedness.

Remark 5.4. The most natural way to find the asymptotics of σ_n would be to estimate the jump discontinuity of the singular functions $\chi_{[a_1,a_3]}g$ and then use

$H_T^* g = \sigma f$. However, the jump discontinuity of $\chi_{[a_1,a_3]} g$ at a_3^- can only be estimated to be of the order $b_3 \cdot \mathcal{O}(\epsilon^{1-2\delta/3})$, where b_3 (see (5.38)) contains the term $e^{K_+/\epsilon}$. Thus, the coefficient in front of the logarithmic term in $H_T^* g$ will also be of the order $b_3 \cdot \mathcal{O}(\epsilon^{1-2\delta/3})$, which results in the useless estimate $\sigma = \mathcal{O}(e^{K_+/\epsilon} \cdot \epsilon^{1-2\delta/3})$. Therefore, it was necessary to replace H_T by the full Hilbert transform H and to consider $Hg = -\frac{1}{\sigma} f$ instead of $H_T^* g = \sigma f$ to obtain the result of Theorem 5.3.

6. Asymptotic analysis for the case of $\sigma_n \to 1$. The previous section described how to derive the asymptotic behavior of the singular values in a neighborhood of their accumulation point at zero.

Here we show how to easily obtain the asymptotic behavior around the second accumulation point equal to 1 using a symmetry property that allows us to exploit the analysis done for the first accumulation point.

We define the operator $H_{T,c} := \mathcal{P}_{[a_2,a_4]} H \mathcal{P}_{([a_1,a_3])^c}$, where $(\cdot)^c$ denotes the complement in $\mathbb{R}$ and $\mathcal{P}$ is the projection operator defined in section 1. Without loss of generality we assume $a_1 < 0 < a_2 < a_3 < a_4$. Consider a singular function $f \in L^2([a_2, a_4])$ of H_T with singular value σ. As it was shown in [1], the spectrum of $H_T^* H_T$ is bounded above by 1. Therefore we can define $\beta^2 = 1 - \sigma^2$ and see that f satisfies the eigenequation

$$f - \beta^2 f = H_T^* H_T f. \tag{6.1}$$

On the other hand we have $H^* H = I$, where H is the full Hilbert transform on the line. Hence f also satisfies

$$f = H_T^* H_T f + H_{T,c}^* H_{T,c} f. \tag{6.2}$$

Subtracting the two equations we obtain a new eigenequation for f, now with eigenvalue β^2:

$$\beta^2 f = H_{T,c}^* H_{T,c} f. \tag{6.3}$$

We will relate this eigenequation to an eigenequation for a different truncated Hilbert problem, obtained by the transformation $x \leftrightarrow 1/x$. Define $\eta = 1/x$ and the singular points $\eta_j = 1/a_j, j = 1, \ldots, 4$. These are ordered as $\eta_1 < 0 < \eta_4 < \eta_3 < \eta_2$. Furthermore, we define the function $\bar{f}(\eta) = \eta^{-1} f(\eta^{-1})$. Note that the support of $\bar{f}$ is $\eta_4 < \eta < \eta_2$. With these notations, we have, noting that $0 \notin (a_2, a_4)$,

$$\begin{aligned} x\,(H_{T,c} f)(x) &= x\,\frac{1}{\pi}\,\text{p.v.}\int_{a_2}^{a_4} \frac{f(y)}{y-x} dy = \frac{1}{\pi}\,\text{p.v.}\int_{a_2}^{a_4} \frac{y\,f(y)}{(1/x - 1/y)}\frac{dy}{y^2} \\ &= -\frac{1}{\pi}\,\text{p.v.}\int_{\eta_4}^{\eta_2} \frac{\bar{f}(\eta)}{\eta - \xi} d\eta = -(\bar{H}_T \bar{f})(\xi) \quad \text{with } \xi = 1/x, \end{aligned} \tag{6.4}$$

where we define the operator $\bar{H}_T : L^2([\eta_4, \eta_2]) \to L^2([\eta_1, \eta_3])$ to be[1]

$$(\bar{H}_T h)(\xi) = \frac{1}{\pi}\,\text{p.v.}\int_{\eta_4}^{\eta_2} \frac{h(\eta)}{\eta - \xi} d\eta. \tag{6.5}$$

[1]In (6.4) we have assumed that the variable transformation in the principal value integrals can be handled in the same way as for ordinary integrals. For a proof of this property we refer to [6, section 3.5].

The range in ξ is obtained from

$$x \in ([a_1, a_3])^c = (-\infty, a_1) \cup (a_3, \infty) \Rightarrow \xi \in (\eta_1, 0) \cup (0, \eta_3) = (\eta_1, \eta_3). \tag{6.6}$$

We now apply the adjoint transform and calculate for $a_2 < z < a_4$

$$\begin{aligned} z\left(H^*_{T,c} H_{T,c} f\right)(z) &= \frac{z}{\pi}\left\{\int_{-\infty}^{a_1<0} + \int_{a_3>0}^{\infty}\right\} \frac{(H_{T,c}f)(x)}{z-x}dx \\ &= \frac{1}{\pi\omega}\left\{\int_{\eta_1}^{0} + \int_{0}^{\eta_3}\right\} \frac{(H_{T,c}f)(1/\xi)}{(1/\omega - 1/\xi)}\frac{d\xi}{\xi^2} \\ &= -\frac{1}{\pi}\int_{\eta_1}^{\eta_3} \frac{(1/\xi)\,(H_{T,c}f)(1/\xi)}{(\omega-\xi)}d\xi \\ &= \frac{1}{\pi}\int_{\eta_1}^{\eta_3} \frac{(\bar{H}_T\bar{f})(\xi)}{(\omega-\xi)}d\xi = \bar{H}^*_T\bar{H}_T\bar{f}(\omega), \end{aligned}$$

where $\omega = 1/z$. We conclude that $\bar{H}^*_T\bar{H}_T\bar{f} = \beta^2\bar{f}$; hence β^2 is an eigenvalue for the truncated Hilbert problem defined by $\eta_1 < \eta_4 < \eta_3 < \eta_2$.

The implication of this result for the asymptotic behavior of the singular values around the accumulation points 0 and 1 is as follows. Consider the case $\beta^2 \to 0$. From the previous section we know that the asymptotic behavior of these eigenvalues (which are the squares of the singular values of $\bar{H}_T$) is given by

$$\beta_n = 2e^{-n\pi\bar{K}_+/\bar{K}_-}(1 + \mathcal{O}(n^{-1/2+\delta})). \tag{6.7}$$

Here,

$$\begin{aligned} \bar{K}_+ &= \int_{\eta_4}^{\eta_3} \{(t-\eta_1)(t-\eta_2)(t-\eta_3)(t-\eta_4)\}^{-1/2}\,dt = (|a_1|a_2a_3a_4)^{1/2}\,K_-, \\ \bar{K}_- &= \int_{\eta_3}^{\eta_2} \{-(t-\eta_1)(t-\eta_2)(t-\eta_3)(t-\eta_4)\}^{-1/2}\,dt = (|a_1|a_2a_3a_4)^{1/2}\,K_+, \end{aligned}$$

where the last equalities can be checked by substituting $t = 1/y$ in the integrals. Using the previous result and recalling the definition $\beta^2 = 1 - \sigma^2$, we obtain the asymptotic behavior in the neighborhood of 1 of the singular values of the original problem defined by a_1, a_2, a_3, a_4.

THEOREM 6.1. *The singular values σ_{-n}, $n \in \mathbb{N}$, accumulating at 1 have the following asymptotic behavior:*

$$\sigma_{-n} = \sqrt{1-\beta_n^2} = \left(1 - 2e^{-2n\pi K_-/K_+}\right)\left(1 + \mathcal{O}(n^{-1/2+\delta})\right). \tag{6.8}$$

7. Comparison of numerics and asymptotics. In the previous sections, the asymptotic behavior of the SVD has been derived. Although these asymptotics hold only in the limit $n \to \infty$, we would like to illustrate that they also yield a good approximation of the SVD for small n. For this, we compare the SVD from the asymptotic formulas with the SVD of a discretization of the operator H_T.

For our example, we choose the points a_i to be $a_1 = 0, a_2 = 3, a_3 = 6, a_4 = 12$ and the discretization $\mathbf{H_T}$ of H_T to be a uniform sampling with 601 partition points in the interval $[0, 6]$ and 901 points in $[3, 12]$. Let vectors X and Y denote the partition points of $[0, 6]$ and $[3, 12]$, respectively. To overcome the singularity of the Hilbert kernel the vector X is shifted by half the sample size. The ith components of the

Table 1
The singular values of $\mathbf{H_T}$ *in the transition from* 1 *to* 0.

$\mathbf{i}$	300	301	302	303	304	305
$\mathbf{s_i}$	0.9942962	0.6630176	0.0397114	$1.1321 \cdot 10^{-3}$	$2.9846 \cdot 10^{-5}$	$7.7106 \cdot 10^{-7}$

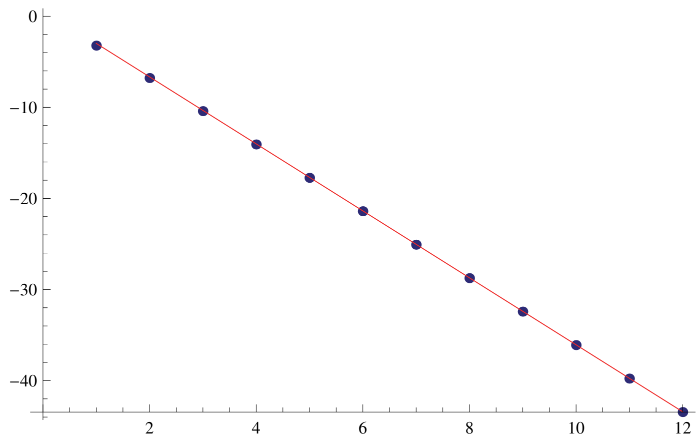

Fig. 5. *Logarithmic plot of the asymptotic (red line) and numerical values (blue dots) of the singular values tending to zero.*

two vectors X and Y are given by $X_i = \frac{1}{100}(i + \frac{1}{2})$ and $Y_i = 3 + \frac{1}{100}i$; H_T is then discretized as $(\mathbf{H_T})_{\mathbf{i},\mathbf{j}} = (1/\pi)(X_i - Y_j)$, $\mathbf{i} = 0, \dots, 600$, $\mathbf{j} = 0, \dots, 900$.

Let $\mathbf{s_i}$, $\mathbf{i} = 0, \dots, 313$, denote the nonzero singular values of the matrix $\mathbf{H_T}$. Table 1 shows a list of a few singular values indicating that for $\mathbf{i} = 0, \dots, 300$ the values $\mathbf{s_i}$ are close to 1, whereas they are close to 0 for $\mathbf{i} = 302, \dots, 313$. Although in theory, 0 itself is not a singular value of H_T but the singular values only decay to 0, they do this at an exponential rate. In practice, this leads to matrix realizations of H_T which effectively have a large kernel.

We compare the singular values $\mathbf{s_i}$, $\mathbf{i} = 302, \dots, 313$, of $\mathbf{H_T}$ with the asymptotic behavior of the singular values σ_n of H_T for $\sigma_n \to 0$ (see Theorem 5.3). Here, we neglect the error terms, i.e., we consider the asymptotic form $\sigma_n \approx 2e^{-n\pi K_+/K_-}$, for $n = 1, \dots, 12$. By shifting the indices $\mathbf{i} = 302, \dots, 313$ the set of indices n that match i are obtained. The value of the shift is found by hand. Figure 5 shows a logarithmic plot of this comparison. While Theorem 5.3 only guarantees that $2e^{-n\pi K_+/K_-}$ is a good approximation of the singular values σ_n for $n \to \infty$, our example demonstrates good alignment already for $n = 1$.

Similarly, we perform a comparison of the singular values $\mathbf{s_i}$, $\mathbf{i} = 293, \dots, 300$, of $\mathbf{H_T}$ with the result from Theorem 6.1 on the asymptotic behavior of the singular values $\sigma_{-n} \to 1$. Again, the error terms are neglected, so that $\sigma_{-n} \approx \sqrt{1 - 4e^{-2n\pi K_-/K_+}}$ for $n = 1, \dots, 8$ is considered instead. A plot comparing $\log(1 - \mathbf{s_i}^2)$ with $\log(4e^{-2n\pi K_-/K_+})$ is shown in Figure 6, illustrating the good alignment for small values of n.

To conclude the numerical illustration, we compare the singular vector $\mathbf{g_{307}}$ of $\mathbf{H_T}$ with the asymptotic behavior obtained for the singular function g_6 of H_T. For this again, only the leading terms in the asymptotic expansions are taken into con-

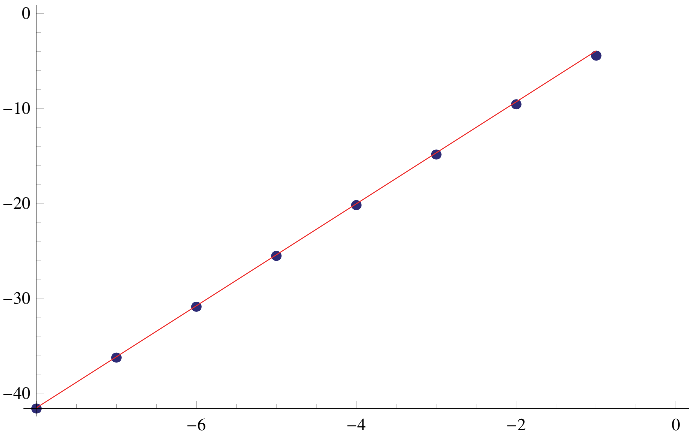

FIG. 6. *Logarithmic plot of the asymptotic (red line) and numerical values (blue dots) of* $1-\sigma_{-n}^2$ *for the singular values* σ_{-n} *tending to* 1.

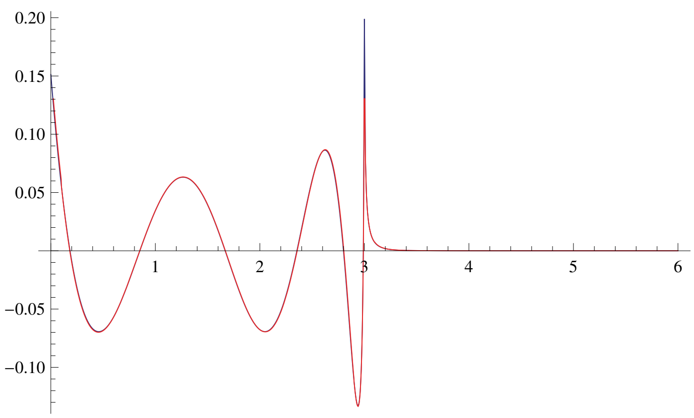

FIG. 7. *The singular vector* $\mathbf{g_{307}}$ *(blue) of* $\mathbf{H_T}$ *compared with the asymptotics for the singular function* g_6 *(red) of* H_T*. Their good alignment makes them hardly distinguishable.*

sideration. To define the approximation to g_6 on the entire interval $[0, 6]$, we first consider the plots of the WKB and Bessel approximations close to a point a_i. Then, the point of transition from the Bessel to the WKB approximation is set by hand at a point of good alignment between the two functions. Figure 7 shows the approximation to g_6 obtained from the asymptotics compared to the singular vector $\mathbf{g_{307}}$. In Figure 8, a logarithmic plot indicates that the asymptotic form is a very good approximation to $\mathbf{g_{307}}$ also on the region where it decays, i.e., on $[3, 6]$.

8. Appendix: Normalization of g on (a_1, a_3).

LEMMA 8.1. *Let* g *be the solution to* $(L-\lambda)\phi = 0$ *derived in section* 5.4*. Then,*

$$\|g\|_{L^2([a_1,a_3])} = \sqrt{\frac{K_-}{2}}(1+\mathcal{O}(\epsilon^{1/2-\delta})). \tag{8.1}$$

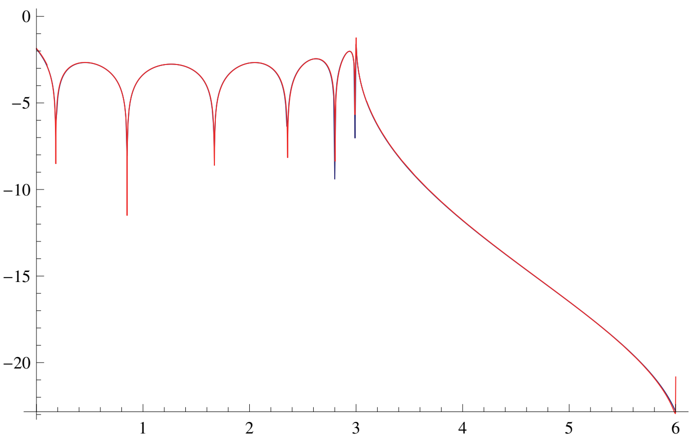

FIG. 8. *A logarithmic plot of the comparison in Figure* 7. *This shows very accurate alignment also in the region* $[3,6]$ *where the functions decay rapidly.*

Proof. We want to determine $\int_{a_1}^{a_3} g^2(x)dx$. The main contribution to this integral comes from the WKB solution (5.26) on $[a_1+\mathcal{O}(\epsilon^{1+2\delta}), a_2-\mathcal{O}(\epsilon^{1+2\delta})]$. We use the abbreviation $\epsilon_\delta := \epsilon^{1+2\delta}$ and derive

$$\begin{aligned}
&\int_{a_1+\mathcal{O}(\epsilon_\delta)}^{a_2-\mathcal{O}(\epsilon_\delta)} g^2(x)dx \\
&\quad = \int_{a_1+\mathcal{O}(\epsilon_\delta)}^{a_2-\mathcal{O}(\epsilon_\delta)} \frac{1}{\sqrt{-P(x)}}\left[\cos^2\left(\frac{1}{\epsilon}\int_{a_1}^{x}\frac{dt}{\sqrt{-P(t)}}-\frac{\pi}{4}\right)+\mathcal{O}(\epsilon^{1/2-\delta})\right]dx \\
&\quad = \int_{a_1+\mathcal{O}(\epsilon_\delta)}^{a_2-\mathcal{O}(\epsilon_\delta)} \frac{1}{\sqrt{-P(x)}}\left[\frac{1}{2}\cos\left(\frac{2}{\epsilon}\int_{a_1}^{x}\frac{dt}{\sqrt{-P(t)}}-\frac{\pi}{4}\right)+\frac{1}{2}+\mathcal{O}(\epsilon^{1/2-\delta})\right]dx.
\end{aligned}$$

The first summand in the integral simplifies to

$$\begin{aligned}
&\frac{1}{2}\int_{a_1+\mathcal{O}(\epsilon_\delta)}^{a_2-\mathcal{O}(\epsilon_\delta)} \frac{1}{\sqrt{-P(x)}}\cos\left(\frac{2}{\epsilon}\int_{a_1}^{x}\frac{dt}{\sqrt{-P(t)}}-\frac{\pi}{4}\right)dx \\
&\quad = \frac{\epsilon}{4}\sin\left(\frac{2}{\epsilon}\int_{a_1}^{x}\frac{dt}{\sqrt{-P(t)}}-\frac{\pi}{4}\right)\Big|_{a_1+\mathcal{O}(\epsilon_\delta)}^{a_2-\mathcal{O}(\epsilon_\delta)} \\
&\quad = \mathcal{O}(\epsilon).
\end{aligned}$$

With that we obtain

$$\begin{aligned}
\int_{a_1+\mathcal{O}(\epsilon_\delta)}^{a_2-\mathcal{O}(\epsilon_\delta)} g^2(x)dx &= \mathcal{O}(\epsilon)+\frac{1}{2}\left(1+\mathcal{O}(\epsilon^{1/2-\delta})\right)\int_{a_1+\mathcal{O}(\epsilon_\delta)}^{a_2-\mathcal{O}(\epsilon_\delta)}\frac{1}{\sqrt{-P(x)}}dx \\
&= \left(\frac{1}{2}+\mathcal{O}(\epsilon^{1/2-\delta})\right)\int_{a_1+\mathcal{O}(\epsilon_\delta)}^{a_2-\mathcal{O}(\epsilon_\delta)}\frac{dx}{\sqrt{-P(x)}}.
\end{aligned}$$

With a Taylor expansion of $1/\sqrt{-P(x)}$, we find that

$$\int_{a_1}^{a_1+\mathcal{O}(\epsilon_\delta)}\frac{dx}{\sqrt{-P(x)}}=\frac{1}{\sqrt{-P'(a_1)}}\int_{a_1}^{a_1+\mathcal{O}(\epsilon_\delta)}\frac{1+\mathcal{O}(x-a_1)}{\sqrt{x-a_1}}dx=\mathcal{O}(\epsilon^{1/2+\delta}).$$

Similarly,

$$\int_{a_2-\mathcal{O}(\epsilon_\delta)}^{a_2} \frac{dx}{\sqrt{-P(x)}} = \mathcal{O}(\epsilon^{1/2+\delta})$$

and thus

$$\int_{a_1+\mathcal{O}(\epsilon_\delta)}^{a_2-\mathcal{O}(\epsilon_\delta)} g^2(x)dx = \left(\frac{1}{2}+\mathcal{O}(\epsilon^{1/2-\delta})\right)\left(K_- + \mathcal{O}(\epsilon^{1/2+\delta})\right) = \frac{K_-}{2}\left(1+\mathcal{O}(\epsilon^{1/2-\delta})\right). \tag{8.2}$$

Let $t = \lambda(a_1 - x)/P'(a_1)$. We consider g in a neighborhood of a_1^+, where it can be represented by $g(x) = b_1 \cdot \hat{\psi}_1(x - a_1)$ for $\hat{\psi}_1$ as in (5.3) for $t \in [0, 1)$ and as in (5.5) for $t \in [1, \mathcal{O}(\epsilon^{2\delta-1}))]$. Using our previous estimate on the coefficient b_1 in (5.24) and a change of variables, we can write

$$\begin{aligned}\int_{a_1}^{a_1+\mathcal{O}(\epsilon_\delta)} g^2(x)dx &= b_1^2 \cdot \Bigg\{ \int_0^1 [J_0(2\sqrt{t}) + \mathcal{O}(\epsilon^{1-2\delta/3})]^2(-P'(a_1)\epsilon^2)dt \\ &\quad + \int_1^{\mathcal{O}(\epsilon^{2\delta-1})} [J_0(2\sqrt{t}) + t^{-1/4}\cdot\mathcal{O}(\epsilon^{1-2\delta/3})]^2(-P'(a_1)\epsilon^2)dt \Bigg\} \\ &= \mathcal{O}(\epsilon)\cdot\Bigg\{ \int_0^{\mathcal{O}(\epsilon^{2\delta-1})} J_0^2(2\sqrt{t})dt + \mathcal{O}(\epsilon^{1-2\delta/3}) \\ &\quad + \mathcal{O}(\epsilon^{1-2\delta/3}\cdot\epsilon^{3(2\delta-1)/4}) + \mathcal{O}(\epsilon^{2-4\delta/3}\cdot\epsilon^{\delta-1/2}) \Bigg\} \\ &= \mathcal{O}(\epsilon)\cdot\Bigg\{ \int_0^{\mathcal{O}(\epsilon^{2\delta-1})} J_0^2(2\sqrt{t})dt + \mathcal{O}(\epsilon^{1/4+5\delta/6}) \Bigg\},\end{aligned} \tag{8.3}$$

where we have used the boundedness of J_0 to simplify the error terms. The asymptotic behavior (5.7), (5.9) of J_0 implies that for some constant c, $|J_0(u)| \le \frac{c}{\sqrt{u}}$, for positive u. With this we obtain

$$\int_0^{\mathcal{O}(\epsilon^{2\delta-1})} J_0^2(2\sqrt{t})dt \le \frac{c^2}{2}\int_0^{\mathcal{O}(\epsilon^{2\delta-1})} \frac{1}{\sqrt{t}}dt = \mathcal{O}(\epsilon^{\delta-1/2})$$

and hence

$$\int_{a_1}^{a_1+\mathcal{O}(\epsilon_\delta)} g^2(x)dx = \mathcal{O}(\epsilon^{1/2+\delta}). \tag{8.4}$$

The part of the L^2-norm of g in the region at a_2^- can be found in a similar fashion. By matching the WKB and Bessel solutions at a_2^- one can find that $b_2 = \mathcal{O}(\epsilon^{-\delta})$ and $c_2 = \mathcal{O}(\epsilon^{-1/2})$ in

$$g(x) = b_2\hat{\psi}_1(x-a_2) + c_2\hat{\psi}_2(x-a_2)$$

for $\hat{\psi}_1$ and $\hat{\psi}_2$ as in (5.3), (5.5) and (5.4), (5.6), respectively. This can also be seen from (5.42), (5.43), since the asymptotic behavior of g at a_2^- can be compared to the one of f at a_3^+. Replacing b_1 by b_2 in (8.3), we obtain similarly to (8.4)

$$\int_0^{\mathcal{O}(\epsilon_\delta)} b_2^2\hat{\psi}_1^2(x)dx = \mathcal{O}(\epsilon^{3/2-\delta}).$$

This yields

$$\begin{aligned}
&\int_{a_2-\mathcal{O}(\epsilon_\delta)}^{a_2} g^2(x)dx = \mathcal{O}(\epsilon^{3/2-\delta}) \\
&\quad + b_2c_2P'(a_2)\epsilon^2\left\{\int_0^1 (J_0(2\sqrt{t}) + \mathcal{O}(\epsilon^{3/2-\delta/3}))(Y_0(2\sqrt{t}) + \mathcal{O}(\epsilon^{3/2-\delta/3}))dt\right. \\
&\quad \left. + \int_1^{\mathcal{O}(\epsilon^{2\delta-1})} (J_0(2\sqrt{t}) + t^{-1/4}\cdot\mathcal{O}(\epsilon^{1-2\delta/3}))(Y_0(2\sqrt{t}) + t^{-1/4}\cdot\mathcal{O}(\epsilon^{1-2\delta/3}))dt\right\} \\
&\quad + c_2^2P'(a_2)\epsilon^2\cdot\left\{\int_0^1 (Y_0(2\sqrt{t}) + \mathcal{O}(\epsilon^{3/2-\delta/3}))^2dt\right. \\
&\quad \left. + \int_1^{\mathcal{O}(\epsilon^{2\delta-1})} (Y_0(2\sqrt{t}) + t^{-1/4}\cdot\mathcal{O}(\epsilon^{1-2\delta/3}))^2dt\right\}.
\end{aligned}$$

The asymptotics of b_2 and c_2 together with the boundedness of J_0 allow us to simplify the above expression to

$$\begin{aligned}
&\int_{a_2-\mathcal{O}(\epsilon_\delta)}^{a_2} g^2(x)dx = \mathcal{O}(\epsilon^{3/2-\delta}) + \mathcal{O}(\epsilon^{3/2-\delta})\left\{\int_0^1 \left|Y_0(2\sqrt{t}) + \mathcal{O}(\epsilon^{3/2-\delta/3})\right| dt\right. \\
&\quad \left. + \int_1^{\mathcal{O}(\epsilon^{2\delta-1})} \left|Y_0(2\sqrt{t}) + t^{-1/4}\cdot\mathcal{O}(\epsilon^{1-2\delta/3})\right| dt\right\} \\
&\quad + \mathcal{O}(\epsilon)\cdot\left\{\int_0^{\mathcal{O}(\epsilon^{2\delta-1})} Y_0(2\sqrt{t})^2dt + \mathcal{O}(\epsilon^{3/2-\delta/3})\int_0^1 \left|Y_0(2\sqrt{t})\right| dt\right. \\
&\quad \left. + \mathcal{O}(\epsilon^{3-2\delta/3}) + \mathcal{O}(\epsilon^{1-2\delta/3})\int_1^{\mathcal{O}(2\delta-1)} \left|Y_0(2\sqrt{t})t^{-1/4}\right| dt + \mathcal{O}(\epsilon^{1/4+5\delta/6})\right\} \\
&= \mathcal{O}(\epsilon^{3/2-\delta}) + \mathcal{O}(\epsilon^{3/2-\delta})\left\{\int_0^{\mathcal{O}(\epsilon^{2\delta-1})} \left|Y_0(2\sqrt{t})\right| dt + \mathcal{O}(\epsilon^{1/4+5\delta/6})\right\} \\
&\quad + \mathcal{O}(\epsilon)\cdot\left\{\int_0^{\mathcal{O}(\epsilon^{2\delta-1})} Y_0(2\sqrt{t})^2dt + \mathcal{O}(\epsilon^{3/2-\delta/3})\int_0^1 \left|Y_0(2\sqrt{t})\right| dt\right. \\
&\quad \left. + \mathcal{O}(\epsilon^{1-2\delta/3})\int_1^{\mathcal{O}(2\delta-1)} \left|Y_0(2\sqrt{t})t^{-1/4}\right| dt + \mathcal{O}(\epsilon^{1/4+5\delta/6})\right\}.
\end{aligned}$$

In view of (5.8) and (5.10), there exists a constant c such that $|Y_0(u)| \leq \frac{c}{\sqrt{u}}$ for positive u. Thus, we obtain

$$\begin{aligned}
&\int_0^{\mathcal{O}(\epsilon^{2\delta-1})} Y_0(2\sqrt{t})^2dt = \mathcal{O}(\epsilon^{\delta-1/2}), \\
&\int_0^{\mathcal{O}(\epsilon^{2\delta-1})} \left|Y_0(2\sqrt{t})\right| dt = \mathcal{O}(\epsilon^{3\delta/2-3/4}), \\
&\int_1^{\mathcal{O}(2\delta-1)} \left|Y_0(2\sqrt{t})t^{-1/4}\right| dt = \mathcal{O}(\epsilon^{1/2-\delta/3}),
\end{aligned}$$

and hence

$$\int_{a_2-\mathcal{O}(\epsilon_\delta)}^{a_2} g^2(x)dx = \mathcal{O}(\epsilon^{1/2+\delta}). \tag{8.5}$$

The last missing piece is the norm of g on (a_2, a_3), i.e., on the region where it is monotonic. Here, we cannot follow the same procedure as before because the results in section 5.2 and the corresponding results in [10] were obtained only on the regions where the solution oscillates.

Instead, we will estimate $\|g\|_{L^2([a_2,a_3])}$ similarly to the derivation in Appendix C in [10]. Let $\{\bar\lambda_k; \bar g_k\}_{k\in\mathbb{N}}$ be the eigensystem of the following Sturm–Liouville problem:

$$L\bar g_k(x) = \bar\lambda_k \bar g_k(x), \quad x \in (a_2, a_3),$$

where the functions $\bar g_k(x)$ are bounded at the endpoints a_2 and a_3. Furthermore, let g_n denote the nth eigenfunction of $\tilde L_S$ obtained from the procedure in section 5.4 and not normalized yet.

Then, $\chi_{[a_2,a_3]} g_n \in L^2([a_2, a_3])$ can be expanded in the orthonormal basis $\{\bar g_k\}$ of $L^2([a_2, a_3])$:

$$\chi_{[a_2,a_3]}(x) g_n(x) = \sum_{k\in\mathbb{N}} \langle g_n, \bar g_k\rangle \bar g_k(x).$$

Let $c_{n,k} = \langle g_n, \bar g_k\rangle$. Then,

$$\begin{aligned}
c_{n,k} &= \frac{1}{\lambda_n}\int_{a_2}^{a_3} (Lg_n)(x)\bar g_k(x)dx \\
&= \frac{1}{\lambda_n}\int_{a_2}^{a_3} (Pg_n')'(x)\bar g_k(x)dx + \frac{1}{\lambda_n}\int_{a_2}^{a_3} 2(x-\sigma)^2 g_n(x)\bar g_k(x)dx \\
&= -\frac{1}{\lambda_n}\int_{a_2}^{a_3} (P(x)g_n'(x))\bar g_k'(x)dx + \frac{1}{\lambda_n}\lim_{\epsilon\to 0^+} Pg_n'\bar g_k\Big|_{a_2+\epsilon}^{a_3} \\
&\quad + \frac{1}{\lambda_n}\int_{a_2}^{a_3} g_n(x)2(x-\sigma)^2\bar g_k(x)dx \\
&= \frac{1}{\lambda_n}\lim_{\epsilon\to 0^+} P(g_n'\bar g_k - g_n\bar g_k')\Big|_{a_2+\epsilon}^{a_3} + \frac{1}{\lambda_n}\int_{a_2}^{a_3} (P(x)\bar g_k'(x))' g_n(x)dx \\
&\quad + \frac{1}{\lambda_n}\int_{a_2}^{a_3} g_n(x)2(x-\sigma)^2\bar g_k(x)dx.
\end{aligned}$$

This implies

$$c_{n,k} = \frac{1}{\lambda_n}\lim_{\epsilon\to 0^+} P(x)[g_n'(x)\bar g_k(x) - g_n(x)\bar g_k'(x)]\Big|_{a_2+\epsilon}^{a_3} + \frac{\bar\lambda_k}{\lambda_n} c_{n,k}.$$

The functions $\bar g_k(x)$ are bounded at the endpoints a_2 and a_3, whereas $g_n(x)$ is bounded at a_3 but has a logarithmic singularity at a_2. Hence, the above simplifies to

$$\begin{aligned}
c_{n,k} &= -\frac{1}{\lambda_n}\lim_{\epsilon\to 0^+} P(a_2+\epsilon)g_n'(a_2+\epsilon)\bar g_k(a_2+\epsilon) + \frac{\bar\lambda_k}{\lambda_n} c_{n,k}, \\
c_{n,k}\left(1 - \frac{\bar\lambda_k}{\lambda_n}\right) &= -\frac{1}{\lambda_n}(a_2-a_1)(a_2-a_3)(a_2-a_4)\phi_{2,n}(a_2)\bar g_k(a_2), \\
c_{n,k} &= C\phi_{2,n}(a_2)\bar g_k(a_2)\frac{1}{\lambda_n - \bar\lambda_k}.
\end{aligned}$$

Here C is constant and, close to a_2, g_n is of the form

$$g_n(x) = \phi_{1,n}(x) + \phi_{2,n}(x)\ln|x - a_2|$$

for analytic functions $\phi_{i,n}$. Furthermore, $g_n(x)$ satisfies the transmission conditions (2.15), (2.16) at a_2 and thus

$$\phi_{2,n}(a_2) = \frac{2}{\pi}c_2 = \mathcal{O}(\sqrt{n}),$$

where we have used $c_2 = \mathcal{O}(\epsilon^{-1/2})$ as in (5.43).

One can also find that $\bar{\lambda}_k = \mathcal{O}(k^2)$ and $\bar{g}_k(a_2) = \mathcal{O}(\sqrt{k})$, similarly to (5.14) and (6.2) in [10]. Note that $\lambda_n \to +\infty$, while $\bar{\lambda}_k \to -\infty$. The norm of $\chi_{[a_2,a_3]}g_n$ can then be found to be

$$\|g_n\|^2_{L^2([a_2,a_3])} = \sum_k c^2_{n,k} = C^2\phi^2_{2,n}(a_2)\sum_k \frac{\bar{g}^2_k(a_2)}{(\lambda_n - \bar{\lambda}_k)^2}$$
$$= \mathcal{O}(n)\cdot\mathcal{O}(n^{-2}) = \mathcal{O}(n^{-1}),$$
$$\|g_n\|_{L^2([a_2,a_3])} = \mathcal{O}(n^{-1/2}). \tag{8.6}$$

Putting together (8.2), (8.4), (8.5), and (8.6), we finally obtain

$$\|g\|_{L^2([a_1,a_3])} = \sqrt{\frac{K_-}{2}}(1 + \mathcal{O}(\epsilon^{1/2-\delta})). \qquad \square$$

Acknowledgment. We would like to thank Ingrid Daubechies for her valuable comments.

REFERENCES

[1] R. Al-Aifari and A. Katsevich, *Spectral analysis of the truncated Hilbert transform with overlap*, SIAM J. Math. Anal., 46 (2014), pp. 192–213.
[2] C. M. Bender and S. A. Orszag, *Advanced Mathematical Methods for Scientists and Engineers* I*: Asymptotic Methods and Perturbation Theory*, Vol. 1, Springer, New York, 1999.
[3] M. Defrise, F. Noo, R. Clackdoyle, and H. Kudo, *Truncated Hilbert transform and image reconstruction from limited tomographic data*, Inverse Problems, 22 (2006), pp. 1037–1053.
[4] A. Erdélyi, *Asymptotic Expansions*, Dover, Mineola, NY, 1955.
[5] D. V. Finch, *private communication*, Mathematisches Forschungsinstitut Oberwolfach, 2002.
[6] F. D. Gakhov, *Boundary Value Problems*, Dover, Mineola, NY, 1990.
[7] I. M. Gelfand and M. I. Graev, *Crofton function and inversion formulas in real integral geometry*, Funct. Anal. Appl., 25 (1991), pp. 1–5.
[8] A Katsevich, *Singular value decomposition for the truncated Hilbert transform*, Inverse Problems, 26 (2010), 115011.
[9] A. Katsevich, *Singular value decomposition for the truncated Hilbert transform: part* II, Inverse Problems, 27 (2011), 075006.
[10] A. Katsevich and A. Tovbis, *Finite Hilbert transform with incomplete data: Null-space and singular values*, Inverse Problems, 28 (2012), 105006.
[11] Q. Kong, M. Möller, H. Wu, and A. Zettl, *Indefinite Sturm-Liouville problems*, Proc. Roy. Soc. Edinburgh Sect. A, 133 (2003), pp. 639–652.
[12] F. Natterer, *The Mathematics of Computerized Tomography*, Classics in Appl. Math. 32, SIAM. Philadelphia, 2001.
[13] F. Noo, R. Clackdoyle, and J. D. Pack, *A two-step Hilbert transform method for* 2*D image reconstruction*, Phys. Medicine Biol., 49 (2004), pp. 3903–3923.
[14] J. D. Pack, F. Noo, and R. Clackdoyle, *Cone-beam reconstruction using the backprojection of locally filtered projections*, IEEE Trans. Medical Imaging, 24 (2005), pp. 1–16.
[15] F. G. Tricomi, *Integral Equations*, Vol. 5, Dover, Mineola, NY, 1985.

[16] Y. Ye, H. Yu, Y. Wei, and G. Wang, *A general local reconstruction approach based on a truncated Hilbert transform*, Internat. J. Biomedical Imaging, 2007. 63634.

[17] Y. Ye, S. Zhao, H. Yu, and G. Wang, *A general exact reconstruction for cone-beam CT via backprojection-filtration*, IEEE Trans. Medical Imaging, 24 (2005), pp. 1190–1198.

[18] T. Zhuang, S. Leng, B. E. Nett, and G.-H. Chen, *Fan-beam and cone-beam image reconstruction via filtering the backprojection image of differentiated projection data*, Phys. Medicine Biol., 49 (2004), pp. 5489–5503.

[19] Y. Zou, X. Pan, and E. Y. Sidky, *Image reconstruction in regions-of-interest from truncated projections in a reduced fan-beam scan*, Phys. Medicine Biol., 50 (2005), pp. 13–28.

[20] Y. Zou and X. C. Pan, *Image reconstruction on PI-lines by use of filtered backprojection in helical cone-beam CT*, Phys. Medicine Biol., 49 (2004), pp. 2717–2731.